Mississippi State University

Scholars Junction

Theses and Dissertations

Theses and Dissertations

8-6-2021

Thermal degradation kinetics of aromatic ether polymers

Keith O. Cobb Jr.
kcobbjr.21@gmail.com

Follow this and additional works at: https://scholarsjunction.msstate.edu/td

Thermal degradation kinetics of aromatic ether polymers

By

Keith O. Cobb Jr.

Approved by:

Dennis W. Smith Jr. (Major Professor)
Dongmao Zhang
Joseph P. Emerson (Graduate Coordinator)
Rick Travis (Dean, College of Arts & Sciences)

A Thesis
Submitted to the Faculty of
Mississippi State University
in Partial Fulfillment of the Requirements
for the Degree of Master of Science
in Chemistry
in the Department of Chemistry

Mississippi State, Mississippi

August 2021

Name: Keith O. Cobb Jr.

Date of Degree: August 6, 2021

Institution: Mississippi State University

Major Field: Chemistry

Major Professor: Dennis W. Smith Jr.

Title of Study: Thermal degradation kinetics of aromatic ether polymers

Pages in Study: 77

Candidate for Degree of Master of Science

Fluorinated polymers of substantial high performance such as perfluorocyclobutyl (PFCB) and fluorinated aryl vinyl ether (FAVE) polymers can readily be synthesized by thermal [2+2] cyclopolymerization as a melt or by classical polycondensation. These fluoropolymers naturally possess high thermal and chemical resistance, low conductivity properties, and other mechanical properties. In this work, a method using 0th order kinetics is proposed and thermal degradation studies were conducted on six different aromatic ether-based polymers to gauge trends in activation energy barrier and differences in thermal stability by 0th order degradation kinetics. The activation barrier (E_a) obtained can give accurate insight into the stability of the polymer based only on structure for external applications. Activation energies ranging from 17 to 41 kcal/mol were obtained for the various polymers. Overall, this study provides an established method using TGA for thermal stability studies through 0th order kinetics that can be potentially used for future lab applications.

DEDICATION

This work is dedicated to my family who never stopped supporting me. I want to give a special thanks to my mother, Cynthia Kirk, and my grandmother, Effie Jean Kirk, who have always been there. I would not have made it this far without them. I also want to dedicate this milestone to my late grandfather, Curtis Ray Crowder, who raised me into who I am today.

ACKNOWLEDGEMENTS

I want to acknowledge my lab mates and colleagues who pushed me to finish. I want to thank all my lab mates in the Smith lab and fellow colleagues. Everyone was such a big help and I could not have done it alone. I also want to thank the people of the Hand Lab Chemistry Department for the wonderful years.

TABLE OF CONTENTS

LIST OF TABLES

LIST OF FIGURES

vii

LIST OF SCHEMES

CHAPTER I

INTRODUCTION

1.1   High Performance Polymer

Polymers are characterized by measuring properties like tensile strength, thermal

resistance, processability, and conductivity. These properties are translated into numerous

applications from general use like styrofoam cups made from polystyrene to more extreme

applications like reinforced carbon fiber composites used in the aircraft industry. The last century

has seen substantial progress in the field of electronics and engineering to match the growth rate

of human population density and related infrastructure. This also means an increase in the

number of materials and tools needed to accomplish everyday tasks. For example, automobile

parts, plane exteriors, engines, pipes, cell phones, and other applications use tough polymers like

Nylon 6,6 or Low-Density Polyethylene (LDE). There are high risk applications for applied

polymers such as in the aerospace industry for vacuum sealing parts, synthetic circuit boards for

electronics, or exterior coating for high temperature environments[1]. These highly stabilized

polymers form a sub-class within the field with high mechanical, thermal, and other notable

properties known as "high performance polymers."

Their production is solely aimed at extreme stress and environmental situations. These

polymers possess a myriad of properties like superior thermal and chemical resistance, high

conductivity, high sound insulation potential, and high mechanical strength. There is a

cacophony of high-performance polymers which include polyetheretherketone (PEEK), polyimides such as poly(4,4´-oxydiphenylene-pyormellitimide) also known as Kapton, and polyethersulfone (PES) (Figure **1.1**).

PES   **PEEK**   **Kapton**
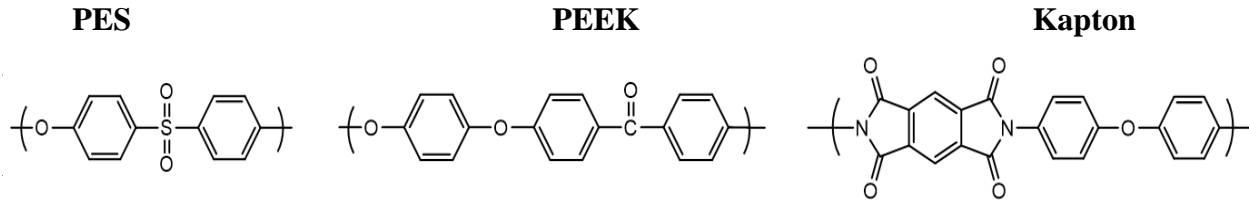
Figure 1.1 Chemical structures of common high-performance polymers

Common high performance polymers left to right: such as Polyethersulfone (**PES**), Polyetheretherketone (**PEEK**), and Poly(4,4´-oxydiphenylene-pyromellitimide) (**Kapton**).[1]

Poly(4,4´-oxydiphenylene-pyromellitimide), Kapton, is a polymer film created by the DuPoint group in the 1960s as a famous high-performance polymer with an expansive range of versatility in regards to temperature. It has a high heat threshold (above 400 °C) and used in the aerospace industry where the high thermal stability is used to support atmosphere reentry. The polymer itself has good dielectric constants aiding to its use for electronic circuits, 3D printing, and manufacturing. PES and PEEK were introduced into the market by Imperial Chemical Industries (ICI) in the 1970's and 80's respectively[2] [3]. PES, an amorphous thermoplastic, is used in its standard form and in a reinforced state. The reinforced PES is intertwined with carbon fiber to increase the mechanical properties for its applications in spacecraft parts. The standard is more daily used as the covering for baking windows as well as processor boards for electronic industry. PEEK, another thermoplastic with a melting temperature of 343 °C is an extremely versatile high-performing polymer. It is also used in aerospace engineering for use in high vacuum environments. Another application is its use as chemical containment within the chemical industry. PEEK is also considered a biomaterial for its applications in the medicinal

field and physical fitness. Through the use of Magnetic Resonance Imaging (MRI) coupled with PEEK can be used to help doctors give patients prosthetic treatment for replacing broken bones or other damaged areas[3]. The same is used for spinal surgery with this thermoplastic imbedded in the patient's spine for recovery[3].

The key characteristic about high-performing polymers is their thermal stability that makes them useful for extreme applications. That being said, the main strength of high-performing polymers is also one of their greatest weaknesses. Kapton, PEEK, and PES are known widely for being thermally resistant which in itself is very useful but this also hinders the commercial process to mold them into proper material. PEEK is a semi-crystalline thermoplastic that has superb mechanical properties but its crystallinity is heavily influenced by the method used. The high melting temp of each of these polymers allows for only certain techniques to be used to properly process them. The conventional use of injection molding is used for PEEK and PES. This method has a preset mold for a material. The applied material is placed inside the molding hot before being left to cool resulting in the finished mold. This is limited to basic industrial patterns and does not have much diversity in 3D shapes[4]. Another way would be to use the extrusion method but the versatility of the desire shapes is limited in that technique. This method uses a linear sheet that has been cut with a pattern. Hot material is sent through this preset cut to form linear sheets of the pattern. This limits the technique to 2D shapes. That problem in itself is a limitation of current high-performing polymers. The cost of some of these polymers also limit their applications in the mechanical industry. PEEK, for example, can be a minimum of $100/kg of material. Kapton can be varied from $25 - $45/kg as well. The price difference between the two means a difference in the scope of applications based on the polymer

economically. The increased cost of manufacturing coupled with the complex processing methods leave a nasty impact on the environment.

1.2 Fluoropolymers

The challenges facing the polymer field have caused a shift in modern materials to include fluorine in the polymer. Polymers containing fluorine atoms are classified as "Fluoropolymers". Varying degrees of these polymers that would normally include Hydrogen are now swapped with varying degrees of fluorine content. Fluoropolymers are used for a variety of applications like chemical treatments, electronics, and mechanical engineering to the same extent or higher than other polymers. Fluoropolymers can also be much less expensive than their counterparts. PolyTetraFluoroEthylene (PTFE), commercially known as Teflon (~22$ per kilogram), is a common fluoropolymer used in everyday house work like cooking pans as well as plastic surfaces for highly acidic solution containment.
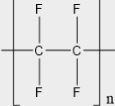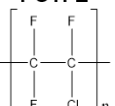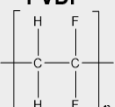
Fluoropolymer	Startup	Melting point (°C)	Tensile modulus (Mpa)	Elongation breakage (%)	Dielectric (kV/mm)	Appl. Temp. (°C)	Applications
PTFE	1947	317 – 377	550	300 – 550	19.7	260	Chemical processing, wire and cable
PCTFE	1953	210 – 255	60 – 100	100 -250	19.7	200	Barrier film, packaging and sealing
FEP	1960	260 – 282	345	~300	19.7	200	Cable insulation
PVF	1961	190 – 200	2000	90 -250	12 -14	110	Lamination, film, and coating
PVDF	1961	155 – 192	1,040 – 2,070	50 -250	63 – 67	150	Coating, wire, cable, electronic insulation
ECTFE	1970	235 – 245	240	250 – 300	80	150	Flame resistant insulation
PFA	1972	302 – 310	276	~300	19.7	260	Chemical resistant components
ETFE	1973	254 – 279	827	150 – 300	14.6	150	Wire and cable insulation
THV	1996	145 - 155	82 – 207	500 - 600	48 -62	93	Barrier film and insulation

Figure 1.2 Table of common fluoropolymers

A comprehensive table of common fluoropolymers and their diverse range of applications.

Fluoropolymers are a class of high-performance materials that are semi-crystalline compounds vastly used thanks to their mechanical properties. Unlike other high-performance materials, fluoropolymers can excel in multiple high-end fields **Figure**. They have high thermal stability and excellent chemical resistance, low dielectric constants for electronic applications, low permeability, low surface energy, and chemical inertness. This is due to the presence of strong fluorocarbon bonds in these polymers versus other high-performing polymers[5].

The use of fluorine instead of hydrogen has many different effects that alter the mechanical and chemical properties for the better. The first notable difference is a difference in strength with the C-H bond energy of 410 (kJ/mol) being significantly weaker than the C-F bonding energy of 450 (kJ/mol) (Table **1.1**).

Table 1.1 Table of bonding energy difference between C-H and C-F bonds

Bond Energies	
Bonds	**Energy (kJ/mol)**
C - H	410
C - F	450

Also due to the dipole moment, low polarizability, and high electronegativity of the fluorine atom, it induces a strong force between itself and carbon. Fluorine is a very small atom with a small radius around its nucleus. The fluorine atom holds onto its electrons tightly so it forms a very strong bond with any atoms bonded to it. This adapts the molecule to be chemically inert to foreign or outside molecules and having a low surface energy, electrical permittivity and refractive index from the fluorine atom[5]. The induction of fluorine started a new category of polymers for a variety of applications from the new chemical and mechanical properties introduced by fluorine. fluoropolymers themselves can be divided into fully fluorinated compounds, where all hydrogens have been replaced with fluorine, and partially fluorinated with some degree of fluorine and hydrogen atoms in the same structure. The difference between the degrees of fluorine atoms affects the mechanical properties as fully fluorinated compounds like PTFE (Polytetrafluoroethylene) and FEP (Fluorinated ethylene propylene) are highly crystalline and more thermally resistant and less friction prone while partially fluorinated compounds like ETFE (Ethylene tetrafluoroethylene) and PVDF (Polyvinylidene fluoride) are more processable and have higher tensile strength[6].

Teflon was discovered by an employee in 1938 at DuPoint Industries on accident before being trademarked in 1945. A researcher was running an experiment with a cylinder of TFE gas and left it unattended. Later when he returned, a waxy white polymer solid was leftover and Teflon was born. Starting with liquid TFE, PTFE can be obtained by radical polymerization and

a suitable initiator like carboxylic acid (COOH). It is a very well-known polymer material with a melting point of ~ 375 °C with incredibly high thermal stability and nonstick surface behavior from a low friction coefficient. The mechanical and electronic behavior of Teflon is owed to the chain of strong C-F bonds as well as the size of Fluorine reducing the wag and bending motions of atoms which in turn reduce the reactivity of the overall polymer leading it to be mainly inert to outside elements.

1.3   Objective

The goal of this project is to establish a method using TGA and 0th order kinetics to effectively study thermal stability of semi-fluorinated polymers and BODA-Ether polymer. The degree of degradation of these fluoropolymers is of interest for use in practical applications. The molecular differences between the polymer structures and mechanical and chemical properties are also studied. Raman spectroscopy studies including spectra observing the crystallinity of the selected polymer were also conducted to better characterize the BODA composites for polymer conversion and analysis for high-risk applications.

CHAPTER II

THEORY AND LITERATURE BACKGROUND

2.1   Semi-fluorinated Poly Aryl Ethers containing Perfluorocyclobutyl (PFCB) Polymers

Cyclopolymerizations of aromatic trifluorovinyl ether monomers can yield a class of fluoropolymer with versatile properties and networks containing the perfluorocyclobutane (PFCB) linkage. There is significant interest in the dimerization of fluoro-olefins as the polymer containing these groups always have enhanced mechanical, thermal, or conducting properties introduced from the fluorine content. The use of such polymers is a step forward in Material Science and can lead to advancement of composites and materials. The synthesis of PFCBs from TFVE groups has been in the literature since the late 90's[7].

The use of Trifluorovinyl ether (TFVE) derived monomers can be used to synthesize unique partially fluorinated high-performance polymers with extreme versatility. PFCBs result from a free radical mediated [2+2] thermal cyclopolymerization of fluoro-olefins to yield fluoropolymers with PFCB linkages with high thermostability and molecular weight compared to others in their category[8]. There are two common methods for preparing of these polymers: Polycondensation (Scheme **2.1**) by basic conditions and free radical mediated thermal [2+2]

cyclopolymerization of trifluorovinyl ether monomers (Scheme **2.2**) as a melt as stated in various literature[9].
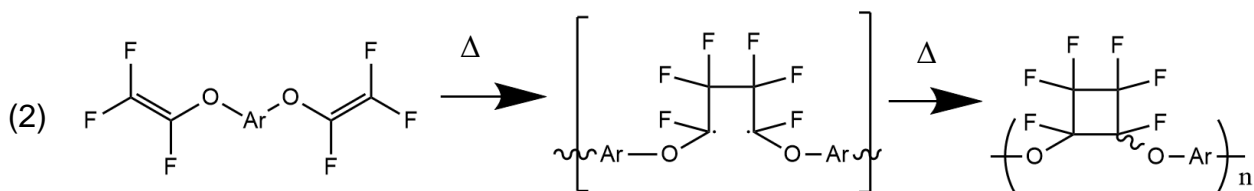
Scheme 2.1 (Thermal cyclopolymerization of trifluorovinyl ether monomers)

Free-radical mediated [2+2] thermal cyclopolymerization of (aryl-bis) trifluorovinyl ether monomers as a melt or in high boiling solvent.[9] Reprinted with permission from (Ref. 10). Copyright (2000) Elsevier. (assessed March 21, 2021)
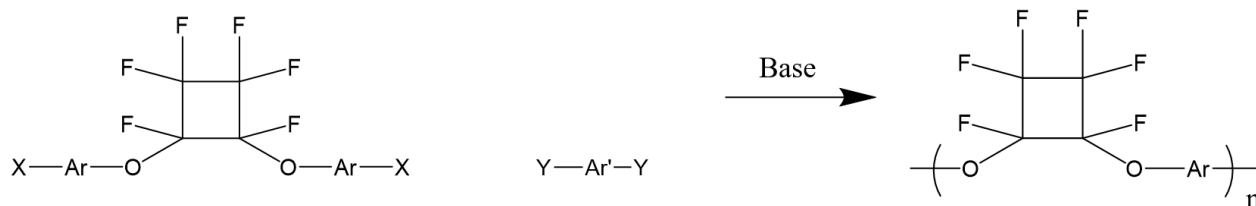
Scheme 2.2 (Classical polycondensation polymerization of perfluorocyclobutyl monomers)

Classical polycondensation of 1,2-bis(aryl ether) hexafluorocyclobutyl halide monomers by use of base.[9] Reprinted with permission from (Ref. 10), Copyright (2000) Elsevier. (assessed March 21, 2021)

These polymers bridge the gap between nonfluorinated polymers with high thermal resistance and mechanical properties and fluoropolymers with chemical resistance, low dielectric constants, and chemical inertness. The existence of the dimerization of fluorinated olefins was discovered back in 1947 at DuPoint in an experiment on the pyrolysis of polytetrafluoroethylene[10].

The discovery of this dimerization behavior of fluoro-olefins was reported in the past literature by Lewis and coworkers at DuPoint through research on polytetrafluoroethylene

9

(PTFE)[10].The perfluorocyclobutane ring formation through thermal dimerization of TFE was uncovered in the 1960s by William Bernett[11]. He studied the molecular orbitals and hybridization behavior of a fluorinated ethylene compound and its hydrocarbon counterpart. He learned that the sp² orbital of the fluoro-olefin had an increase angular strain in comparison to the sp² orbital of hydrocarbon ethylene (Figure **2.1**). The fluoro-olefin is sometimes considered a sp³ diradical leading to an increase in strain as the increased electron density leads to more electron repulsion. This is alleviated as angular strain decreases by ~ 9 kcal/mol after PFCB ring formation. The hydrocarbon, on the other hand, increases only slightly going to the ring formation energy level. This gives us insight into the driving force behind PFCB ring formation as the energy difference observed is more thermodynamically favored.
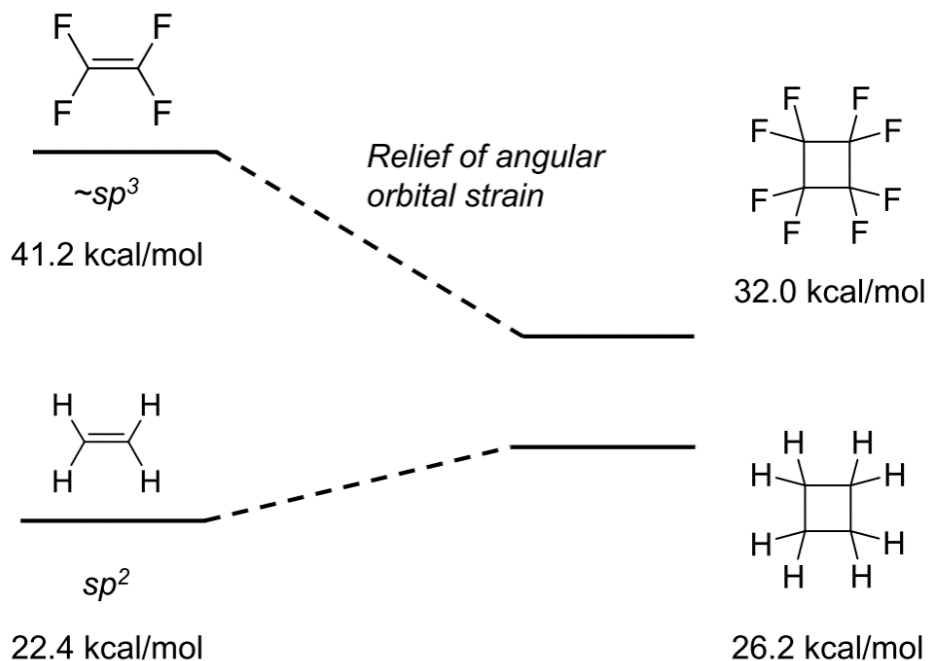
Figure 2.1 Orbital diagram comparison of strain energy from the dimerization of ethylene to the PFCB ring

Energy diagram comparison of strain energy between the dimerization of fluorinated ethylene versus its hydrocarbon counterpart to the perfluorocyclobutane ring.[12]

The activation energies for the cyclizations of the olefins to the PFCB ring were also reported. They noted a forward activation energy of 25.4 kcal/mol versus the reverse reaction of 74.1 kcal/mol[13] [14]. The difference in reaction energy in favor of the forward reaction supports the theory that the ring formation is more thermodynamically favored for the olefin to cyclodimerize[15] [13]. Another benefit from thermal cyclopolymerization is that it can proceed in high boiling solvent or as a solid induced heat with no outside chemicals or additives are required.

Perfluorocyclobutyl aryl ether polymers were introduced to a wide audience in the 1990s by Dow[7]. But the first of its commercial kind was reported in 1968 by Richard Beckerbauer[16]. He gave the world its first high molecular weight PFCB containing polymer from cycloaddition of fluoro olefins using perfluoroalkyl monomers. The change in chemical properties from fluorine increases the versatility and value of such polymers. They are also more processable compared to other polymers. Available precursors and simple procedures may offer PFCB polymers to be more economically favored as well[17].

2.2   Semi-fluorinated Poly Aryl Ethers containing Fluorinated Arylene Vinyl Ether (FAVE) Polymers

Fluorinated arylene vinylene ether, or FAVE, polymers possess unique properties that may enable them to be used as additives and coatings in complex applications for high-performance materials and electronics[18]. Fluorinated arylene vinylene ether containing polymers have a unique attribute to be dual functional. This allows the polymer containing this linkage to further propagate or crosslink with another polymer because of reactive end groups on both dual ends of the polymer chain. Scott Iacono, them at Clemson University, reported the first synthesis of these derivatives of fluoropolymers [19]. There it was proven to be possible to

produce fluorinated aryl ether polymers by step-growth reaction of commercial

bis(trifluorovinyl) aryl ether polymers with bisphenols by use of a base such as sodium hydride

(NaH) in Dimethylformamide (DMF) at 80°C (Scheme **2.3**).
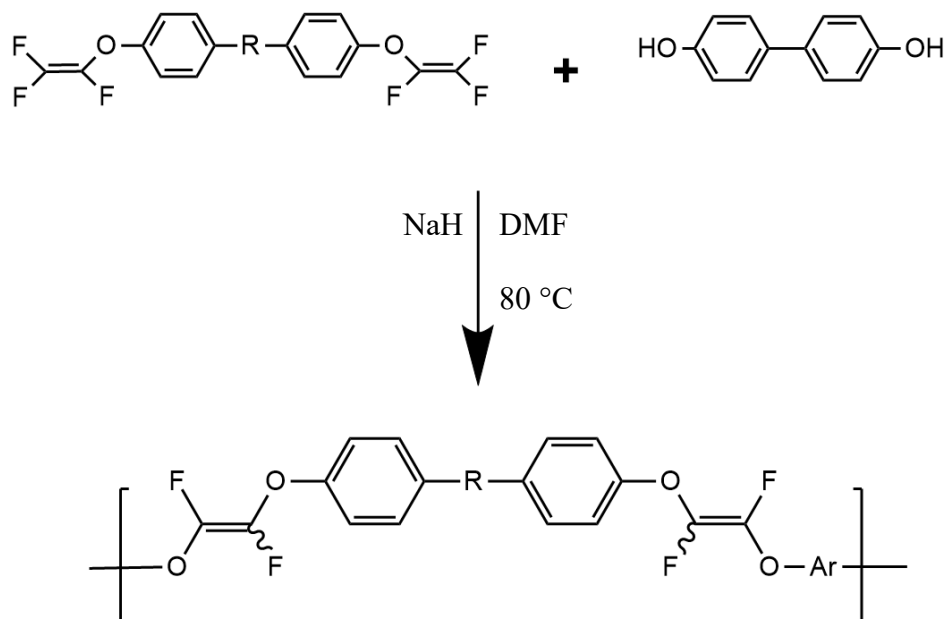
Scheme 2.3 (Fluorinated Aryl Vinyl Arene synthesis route using bisphenols)

General synthesis of FluroinatedAryleneVinylEthers (FAVEs) by base (NaH) catalyzed step-growth polymerization.[18] Reproduced with permission from (Smith et al.; Advances in Fluorine-Containing Polymers). Copyright (2012) American Chemical Society. (assessed March 21, 2021)

The resulting polymers were telechelic so the chain could be selectively propagated by

the presence of reactive end groups. The presence of olefin end groups enables selective control

over the degree of chain propagation by inducing TFVE cyclopolymerization at 210 °C. There is

also potential for further polymerization means by increasing the fluoro-olefin concentration

inside the polymer[18]. Due to this massive increase in olefin content, there is now also potential

to crosslink the polymer at higher temperature >325 °C. The chain propagation and crosslink

potential define the dual functionality of FAVE polymers that make them more versatile and potentially valuable compared to other fluoropolymers in the same class.

2.3   Kinetics by TGA

The thermal stability of a polymer is one of the key characteristics studied and reported for a polymer. One way the thermal stability of a polymer is measured is by identifying the temperature where dramatic weight loss becomes apparent in a dynamic heating experiment. It is of critical interest to find the peak temperature the polymer can handle and the rate of degradation in different environments for practical applications. Scientists observe the thermal stability of polymers by use of Thermogravimetric Analysis (TGA). TGA enables us to place a sample in a small isolated furnace of known nitrogen, air, or other pure or mixed atmosphere and induce heating over a given period of time and rate. The TGA technique can be divided into dynamic heating and isothermal heating. For a dynamic experiment, the heat is raised at a constant or changing rate and the rate of weight loss changes are measured with temperature. For an isothermal experiment, the heat is held at a constant temperature over the specified timespan and the rate weight loss is constant. The data is obtained at the end of the time interval and allows us to view the rate of change a sample's weight %, starting from the initial concentration over the given period (Figure **2.2**).
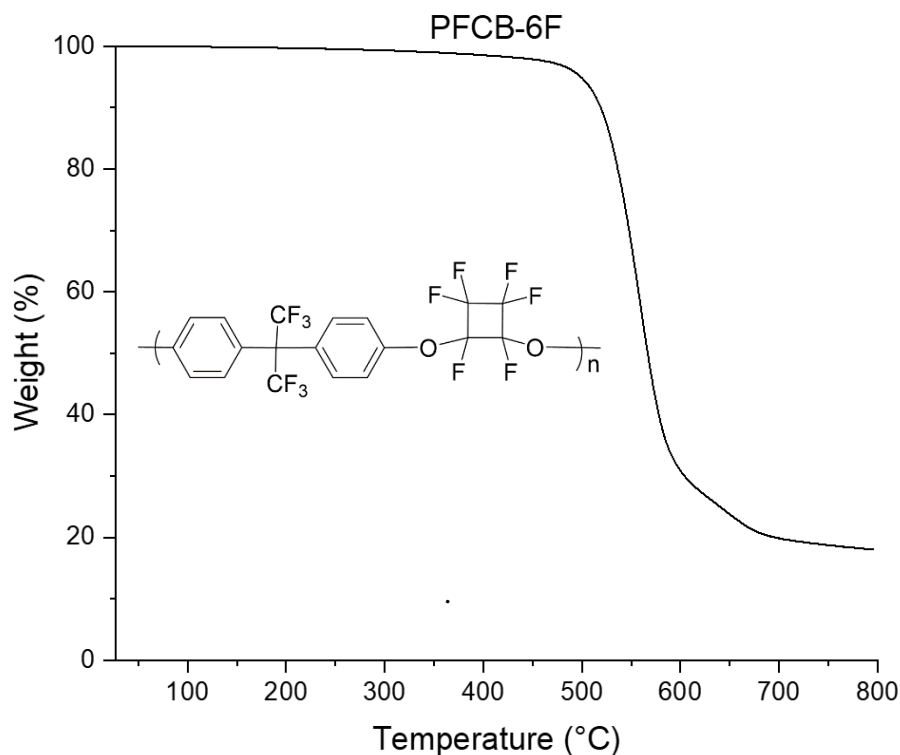
Figure 2.2 Dynamic TGA spectrum of PFCB-6F

An example dynamic TGA spectrum of PFCB-6F heated 10 °C/min from 25 °C to 1000 °C.

The y-axis is usually "Weight Percent". The x-axis is usually "Temperature" for dynamic heating experiments and "Time" for isothermal heating experiments. The general method used for TGA is dynamic heating that gives you weight loss as a function of temperature. A sample is placed into the TGA and is heated at a consistent rate (e.g., 5 °C/min, 10 °C/min or 20 °C/min). In these experiments, the weight loss change depends on the temperature. Thermal stability of a polymer at a constant temperature can also be studied. However, for an isothermal experiment, the heating rate is kept at a constant so the weight loss is now dependent on the rate of degradation itself at that temperature. This lets us look at the sample and note changes at key timestamps over the interval to note early decay or bond breakage before or after the time interval for observance under constant heat **Figure 2.3**. This can be related to thermal stability as

14

to how prone the sample is to losing weight at a certain temperature. TGA can be also used in polymer chemistry to find the temperature dependent rate constant and then the activation energy of a polymer sample. In this work, the isothermal heating method is used.
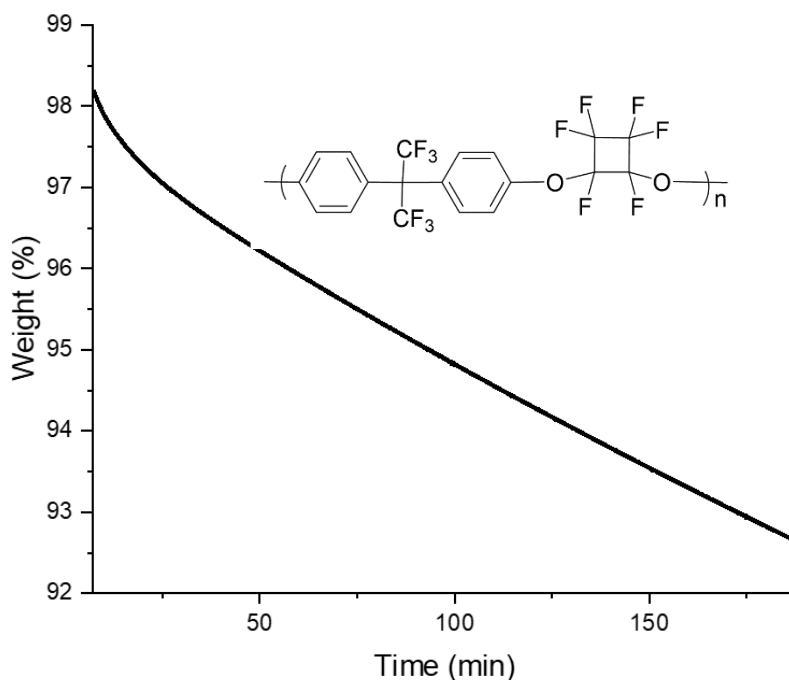
Figure 2.3 Isothermal TGA spectrum of PFCB-6F at 400 °C

An example isothermal TGA spectrum of PFCB-6F heated at 400 °C at a constant rate for 3 hours.

The rate constant "k" of an observed spectrum can be obtained from different methods. Dynamic TGA or conventional TGA experiments commonly use the Flynn and Wall method[20]. This commercial method is used to determine the rate constant using three separate runs at different heating rates for the selected sample. Isothermal TGA experiments could use a method developed by Sorenson in 1978[21]. This method defined a constant heating rate for the sample and two weight loss per min thresholds to gauge the weight loss rate. Those are just a few examples of the many methods derived from TGA to determine the rate constant. Isothermal TGA is readily used to relate the decomposition rate to activation energy. By isothermal TGA,

15

kinetics and activation energy are readily intertwined so it infers that you can also get activation energy from the rate of weight loss (%/t) for a given sample. Using the theory of rate kinetics, it is possible to find the activation energy from the weight change percent of a given polymer sample over a set temperature range. Rate orders consist of zeroth, first, and second order rates. Zeroth order rates laws are the most closely related to direct weight loss to rate and time[22]. Zero-order kinetics enable us to bridge the gap between rate and activation energy.

The polymer structure dependent activation energies for thermal degradation obtained in this work are aimed at quantifying degradation kinetics of the given fluoropolymers and establish a general method through TGA. Degradation itself is the degrading or wearing a way of a material over a time interval and under pre-set conditions. From a chemistry standpoint, degradation is the breakdown of larger molecules into smaller molecules over time by the surrounding environment or other sources. Heat is used in this case for the sample over time in an isolated atmosphere. Thermogravimetric Analysis is the technique used to find the activation energy of a polymer. The activation energy obtained from degradation is related to the rate of sample weight loss per hour while in a given atmosphere.

In a zero-ordered reaction, the rate is independent of concentration (Equation **2.1**)

$$rate = -\frac{[d]A}{[d]t} = -k$$

(2.1)

The rate law conveys the theory that a plot of reactant concentration as a function of time would yield a straight line with a negative slope. The "k" representing that negative slope equals the rate constant for a reaction as the concentration "A" decreases at a consistent pace since reactant is used up in order to form products. The opposite is true in relation to the plotting of

product concentration as a function of time "t". The concentration would increase over the course of the reaction as more product forms. For the zero-ordered rate law above, the rate constant, the reactant concentration, and the time are the only variables. However, because this is zero-ordered the concentration is not of interest when related to the rate constant as it is unaffected by sample concentration. This leaves the rate and time variables. Rate and time can be intertwined to study the effects on weight loss for a given sample. The theory behind sample degradation in inert atmosphere is that weight % is directly related to rate in a time interval (Equation **2.2**).

$$\% \, weight = kt$$

(2.2)

The equation does not consider the concentration of the polymer sample in regards to the rate of decomposition. This is similar to zero-ordered behavior and can be used in conjunction with the collision theory and the Arrhenius law to observe both the rate constant and the kinetics of degradation of fluorinated polymers leading to the calculation of activation energy. In order to obtain activation energy hidden within the spectra, the use of the Arrhenius law (Equation **2.3**) in tandem with zero-order kinetics is pivotal.

$$k = Ae^{-E_a/RT}$$

(2.3)

The Arrhenius law observes the relation of temperature on reaction rate and calculation of activation energy from the equation or the Arrhenius plot. In this case, the Arrhenius plot is used in which the Arrhenius law is adapted into a linearized version of itself in a graph of the logarithm of rate constants versus inverse temperature for the sample observed. The linearized

Arrhenius law can also be seen as another form of the slope intercept formula ($y = mx + b$). The graph shows an x-axis for logarithm concentration and the y-axis is the reciprocal of the temperature (Figure **2.4**).
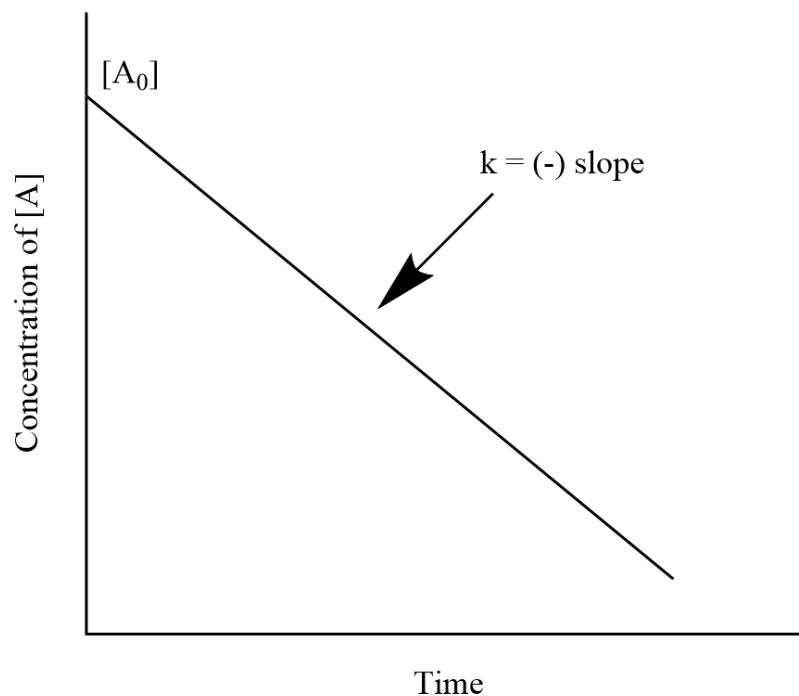
Figure 2.4 Theoretical 0th Order plot for a sample in a reaction.

Theoretical plot of a zero-ordered reaction with the sample concentration decreasing as a function of time.

The negative slope result seen from the data plotted gives a straight line representing "k" for rate constant as well as activation energy for the sample at constant temperature. Using the slope intercept formula, we can relate the two concepts and obtain activation energy from the Arrhenius plot of the TGA spectra of the observed rates for the samples at observed intervals of time at constant temperature. The zero-ordered plot and Arrhenius plot relate similarly by plot behavior so using what is known about zero-order reactions, we can notice other physical aspects

18

of our polymer matrix. The degradation showcased in the graph is independent of concentration per zero-order theory. Thus, in relation to the fluoropolymers, would give us the rate and activation energy based on the rate of degradation as a function of the polymer matrix structure and intermolecular forces that govern stability and behavior of the monomers that were used to produce the polymer.

Based on a report from Dow in the late 1990s, the relationship between zero-order kinetics and activation energy can be obtained by use of the Arrhenius plot (Figure **2.5**)[22]. They studied x-linked or network based PFCB polymers by TGA and isothermal degradation over an ~100 ° range from 300 °C – 400 °C. The study was to probe the effect of substitution of "x-linker" of a triaryl phosphine oxide-based polymer versus a triaryl methyl-based polymer. They were studied under air and nitrogen separately. Experimentation under air caused degradation diverting from zero-order concepts so nitrogen was taken only. They reported an activation

energy of 52 kcal/mol for the fluoropolymer. This study provided potential for future studies of

other fluoropolymers for the advanced characterization in the high-end polymer field.
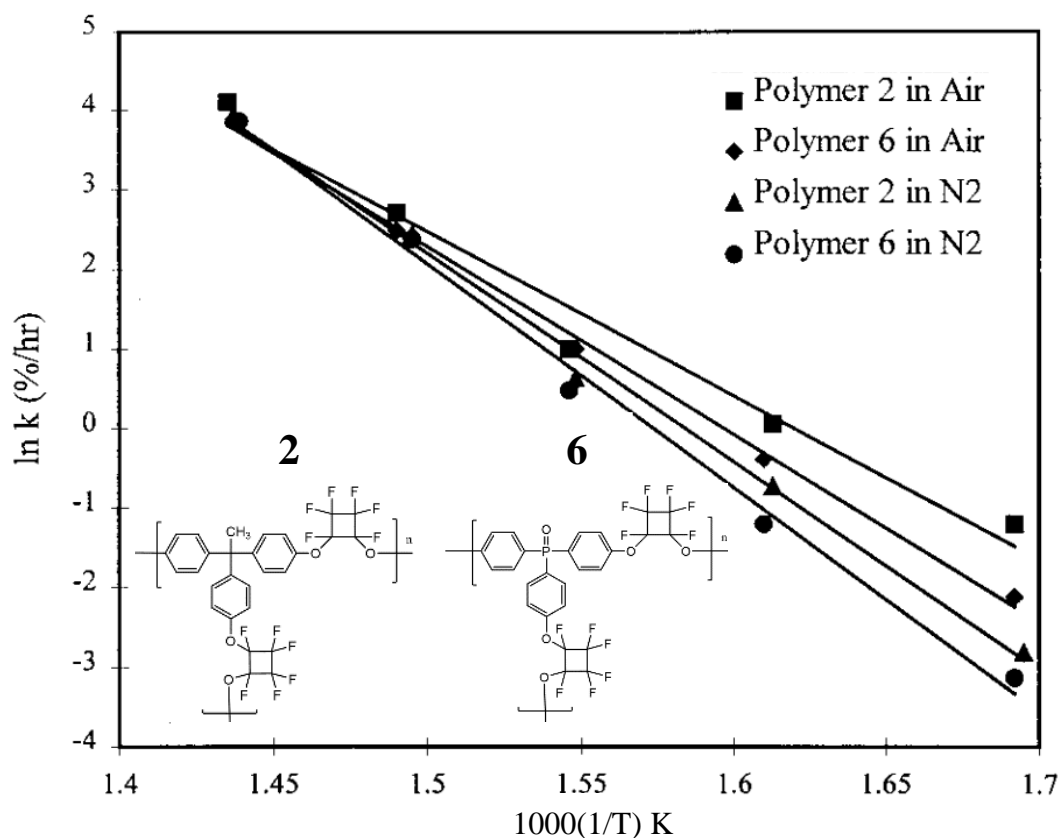
Figure 2.5 Arrhenius plot

Arrhenius plot of compared PFCB polymers under study in the literature.[22] Reproduced with
permission from (Ref 17). Copyright (1998) John Wiley and Sons. (assessed March 10, 2021)

2.4   Raman Spectroscopy

Raman Spectroscopy is an analytical technique that can be used to identify a compound

based on its structure or morphology. Raman can be used to fully characterize and identify

critical regions of a sample like its structure, vibrational interactions of functional groups and

crystallinity of polymeric samples. It is complementary to IR spectroscopy. The use of both in

tandem can clearly characterize a polymer by backbone identification by Raman and

identification of side functional groups by IR. Raman spectroscopy works by hitting a sample with a laser source and recording the signal from the photons scattered by the sample. Most of the scattered incident light that hits the sample is the same wavelength as the light source so it is not usable and that phenomena is called Rayleigh Scattering. However, a small percentage of scattered light is of a different wavelength and the wavelength depends on the chemical structure of the sample itself. This scattered light phenomenon is called Raman Scattering and is used readily today to understand the morphology and crystallinity of polymers for potentials applications in material science.

Raman spectroscopy is very useful for characterizing high-performance polymers. It can be used to follow a sample through polymerization to a completed polymeric product. It has been reported by Smith at Dow in a study observing the detailed kinetics of trifluorovinyl ether polymers following a sample from monomer to oligomer to fully cured through Raman spectroscopy (Figure **2.6**)[9].
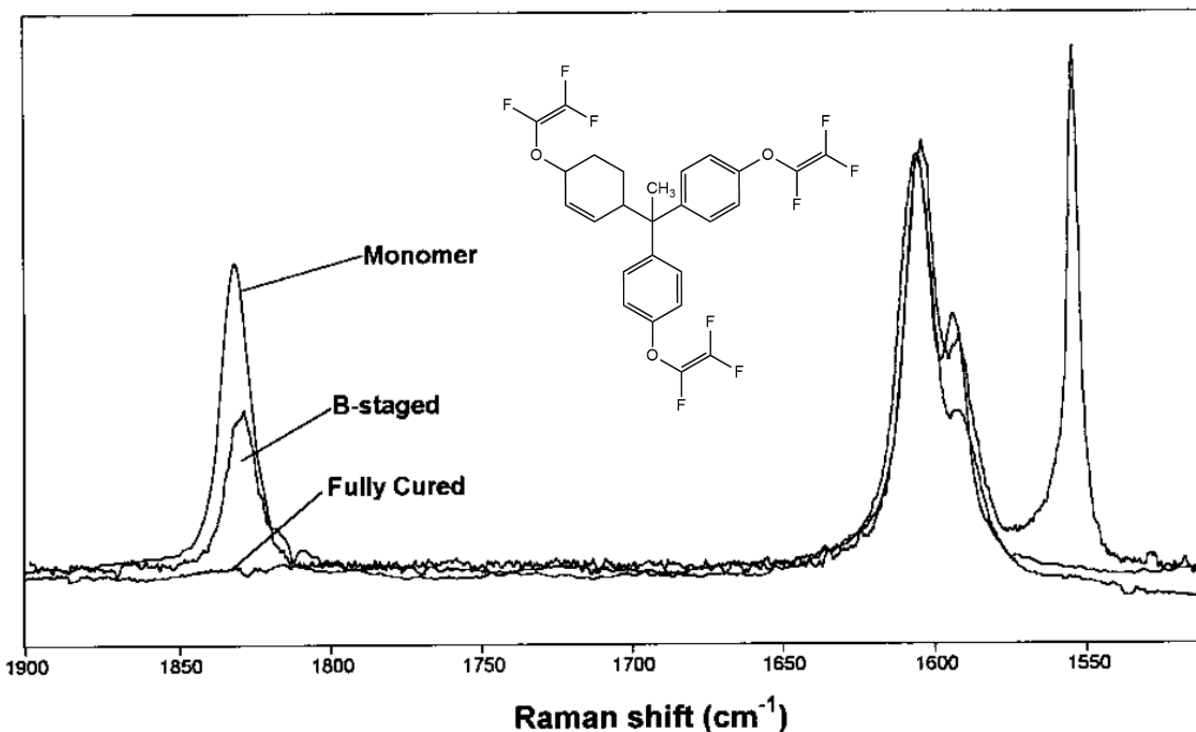
Figure 2.6 TVE Raman spectra

A stacked Raman spectrum following TVE monomer as it fully converts to polymer.[9]
Reprinted with permission from (Ref 10). Copyright (1998) Elsevier (assessed March 21, 2021)

The Raman spectrum showed different states of conversion for the TVE monomer as it is

heated until fully cured. They obtained detailed bands around 1831 cm^{-1} belonging to

fluorinated C=C stretching specific to TFVE chain groups. The degree of intensity of the band

decreases as the monomer is polymerized to oligomer and further cured until no end groups

react. This shows through the use of the Raman spectroscopy technique a sample can be

thoroughly identified at each stage of the polymerization process.

Raman spectra is also used to verify the composition of a polymer sample. The vibrations

and interactions between substituents and the polymer chain as the sample cures is of interest.

Carbon composites like carbon fibers and graphite are used in different applications for high

performance polymers. In glassy carbon or graphitic structures, the rigid network of polycyclic rings is one of the key characteristics of carbon products[23]. Ideas of using these carbon-based materials or other similar polymers in order to crosslink or to get a novel polymer has been of interest. A study in the literature observed nanocomposites of polyacrylonitrile based carbon fibers for analysis at different excitations and band identification of noticeable vibration peaks[24]. The PAN carbon fibers have a significant amount of graphene like structure which can be seen as "G" and "D" band peaks ($\sim 1610\ cm^{-1}$ & $\sim 1320\ cm^{-1}$) associated with graphene that were identified in the PAN fibers as well (Figure **2.7**)[25]. Raman can be applied to identify the vibrational peaks inside the sample and compare the observed peaks to pure carbon fibers. The "G band" is representative of the C=C interactions that make up a large percentage of intermolecular interactions in the polymer matrix. The sample observed seems to retain the graphene like stacking when carbonized to some degree with a broad disorder band (D band). The broadness is linked to varying degrees of disorder or conversion as the sample is carbonized. The D band decreases as the sample is closer to being fully carbonized and the apparent size is

relative to polymer conversion or other atoms hindering the stacking process to fully cured product.
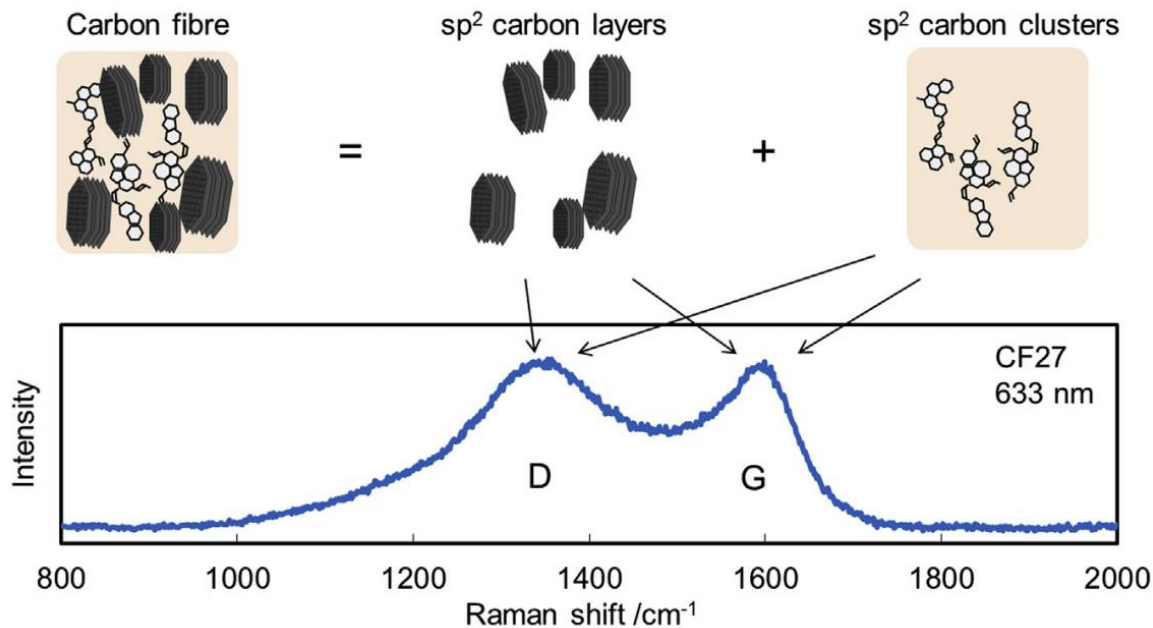
Figure 2.7 Raman peak assignment

"D" and "G" peak assignment of Polyacrylonitrile (PAN) based carbon fibers.[24] Reprinted with permission from (Ref 20). Copyright (2018) Elsevier (assessed March 21, 2021)

It is possible to gain an incredible amount of data from a polymer using Raman spectroscopy. Changes in chemical structure and percentage of crystallinity are just a couple of ways but those two are critical to the future of polymer science. Raman is used in this work for the characterization of a novel carbon-carbon composite, BODA, at different cure stages. For the future development of high-performing polymeric materials, the several interactions that govern the surface morphology of these polymers need to be thoroughly investigated for careful determination of high-performance applications.

CHAPTER III

MATERIALS AND EXPERIMENTAL METHODS

3.1 **Materials**

Commercially available **P1** (PFCB-6F) and **P2** (PFCB-BP) polymers were graciously

donated from Tetramer technologies, LLC, Pendleton, SC. The other polymers (**P3-P6**) were

synthesized by the Smith group as per the literature and donated by name for study.

3.2 **Thermogravimetric Analysis (TGA)**

TGA analysis was conducted using a TA instrument Q50 for degradation studies. The

sample sizes ranged from 5 to 15 mg. For polymers, the samples were heated at a constant rate of

10 °C/min from 25 °C to desired temperature and held for 3 hours. For monomer samples, they

needed to first be heated to polymerization then studied using the isothermal method. The

monomers of a sample were heated to 250 °C then held there for 2 hours to fully polymerize

before heating to experiment temperature. The BODA-Ether sample was heated to 250 °C and

held for 1 hour, then heated to 400 °C and held for 1 hour before finally going to experimental

temperature. The BODA-Ether polymer samples were then further cured by heating to max range

for the TGA instrument (900 - 1000 °C) to get final carbon stage for isothermal experiments.

The rate (k) can be obtained by changing the x-axis from "temperature" to "time". This

will give us the weight loss over time as needed for isothermal studies. The samples were heated

at a constant rate over a 3-hour period. The samples were ran twice on average at the specified

25

temperature in the TGA to get the average rate. The rate itself is given in % of weight loss/3 hr. We can then find the rate constant in (%/hr.) from this spectrum. The standard deviations of the rate constants vary with the temperature. Each polymer sample was heated in a set 100 °C temperature range specific to the individual polymer. The lower end of the temperature range had a lower degree of deviation compared to the higher end for the polymers. This is most likely a result of dramatic degradation at the higher end of the selected temperature range. The statistics and parameter for each polymer is given in Appendix **A.2**.

3.3   Raman Characterization

Raman spectra were acquired with ~ 13 mW laser power. All Raman spectra were acquired using an Olympus 10x objective (NA = 0.25) and the spectrograph grating was 600 grooves/mm. The acquisition times for normal Raman spectra were varied between 20 and 100 s. The Raman shift was calibrated with a neon lamp. Raman shift accuracy was ~ 0.5 cm^{-1}. Reflective sample substrate (RSS) slides from Raminescent, LLC were used for the Raman acquisitions. These RSS slides are highly reflective substrates with negligible fluorescence and Raman background.[26]

CHAPTER IV

RESULTS/ DISCUSSION

4.1   Degradation Kinetics

TGA was used to observe the thermal degradation kinetics for the six different polymers. Polymers (**P1** – **P6**) (Figure **4.1**) were heated 10 °/min from 25 °C to 1000 °C under N_2 atmosphere. An overlay spectrum of the studied polymers is given (Figure **4.2**). These polymers were also heated isothermally for 3 hours at fixed temperature ranges and showed linear weight loss slopes that yield the 0th order rate constant "k" in units of %/min or %/h. Temperature dependent 'k' was then used to obtain activation energies ranging from 17 – 41 (kcal/mol) for the selected polymers. The Arrhenius plots for each polymer was also plotted (Figure **4.3**).
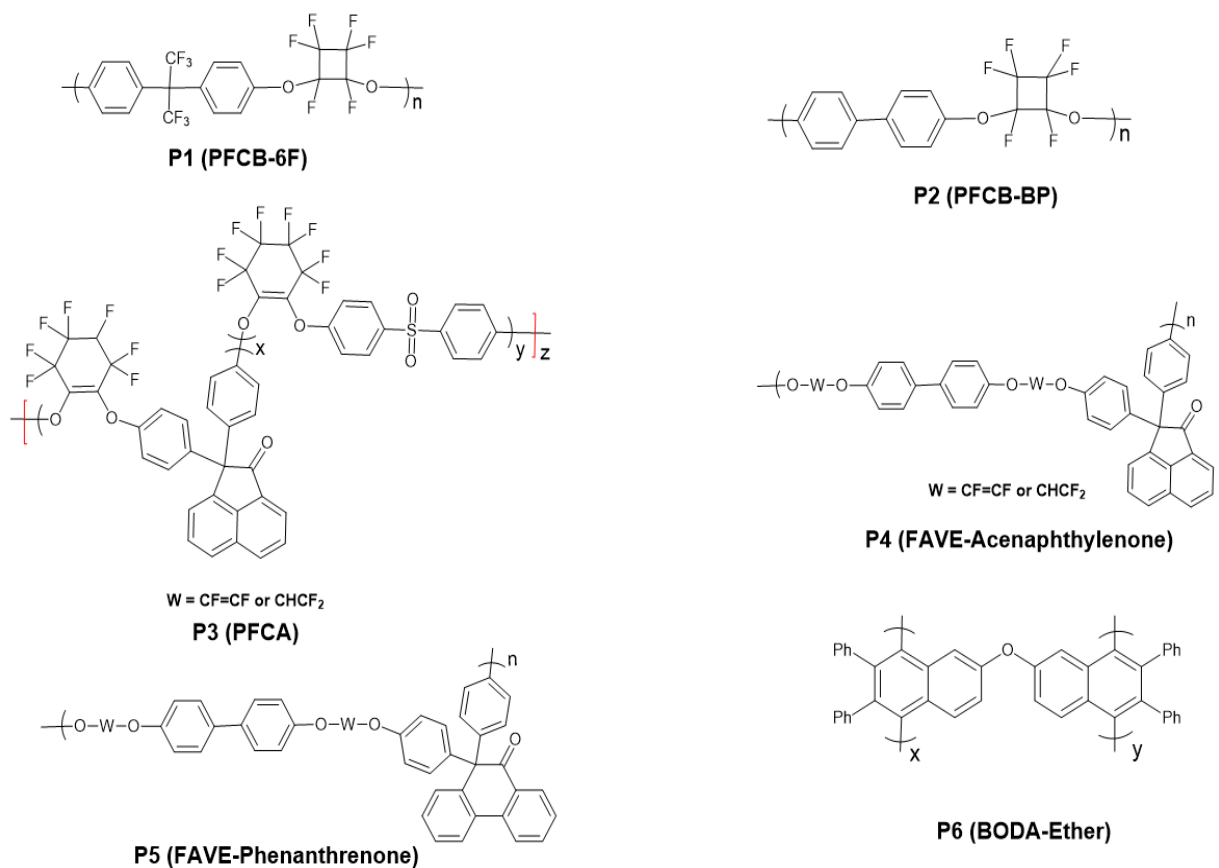
Figure 4.1 Structures of the selected Polymers

Chemical structures for the selected polymers.
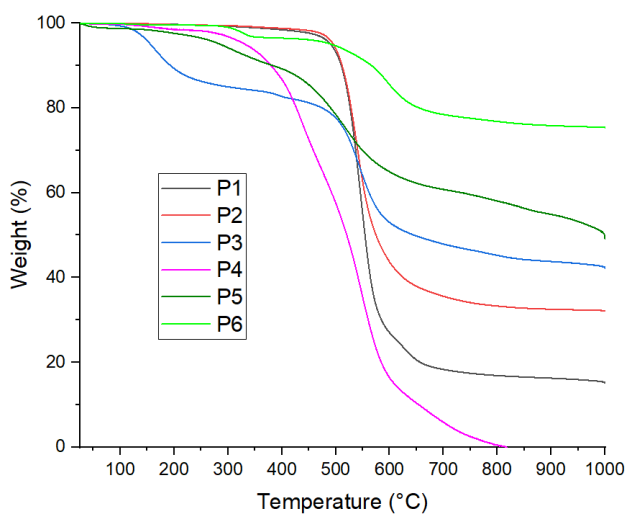
Figure 4.2 Overlay TGA spectrum for the selected polymers

An overlay TGA spectrum of the selected polymers heated from 25 °C to 1000 °C at a heating rate of 10 °C/min
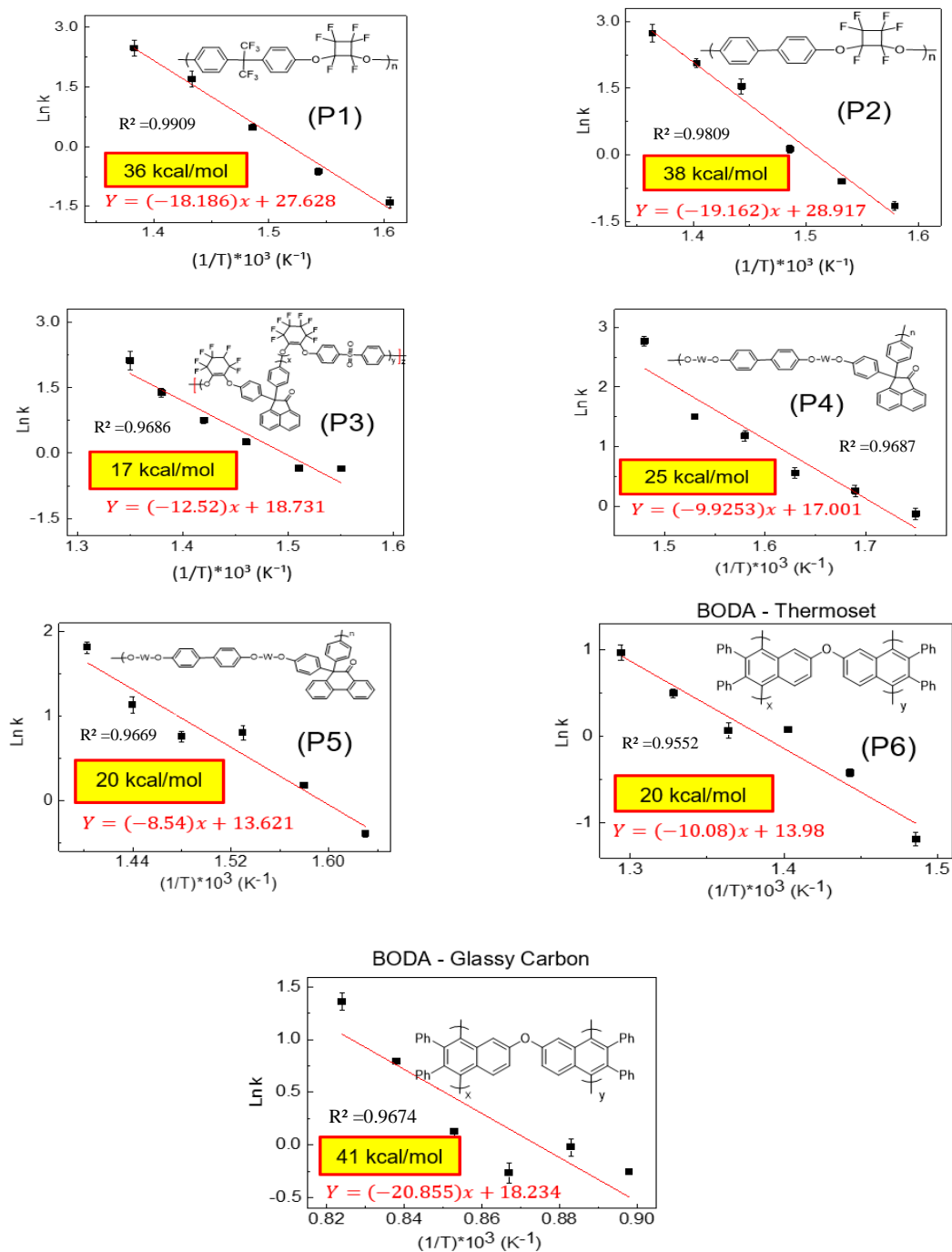
Figure 4.3 Arrhenius plots on average rates

Arrhenius plots for the selected polymers based on the average degradation rate over the 3-hr. isothermal experiment.

Analysis into the trend of activation energy was also undertaken (Figure **4.4**). The

Arrhenius plots for each polymer also shed some light on the stability of the samples as they are

heated. The slopes of each line are used to find the activation energy. There were slight deviations of ± 1 for each slope. The data cluster for some of the polymers were more deviated than others. **P1 – P3** showed little deviation from the trend line compared to polymers **P3 – P6** that showed more deviation. This deviation can be linked to reactivity of the sample at the specified temperature. All polymers undergo drastic degradation at different temperatures. It is possible the temperature range used went past this temperature for some of the polymers and caused large shifts in degradation rate that causes it to be an outlier comparison to the other data points. Some of the polymers exhibit similar behavior as can be seen on the overlay spectrum. This leads to characterization into groups like PFCB based or FAVE based for the selected polymers. Heat was the only variable applied as the behavior of zero-ordered rates were independent of concentration so structure of the polymers is the key to understanding the trend of activation energy and concept of thermal stability. There is a notable trend among the activation energies of the selected polymers distinguishing them by their structure or functional spacer.
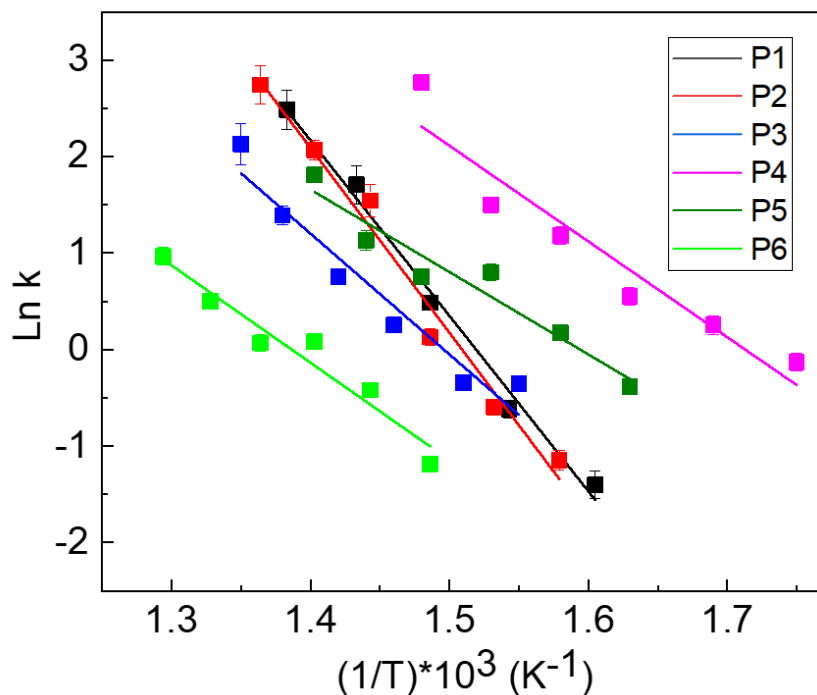
Figure 4.4 Overlay Arrhenius Plots

An overlay of the Arrhenius plots of the selected polymers. (BODA as thermoset only)

Starting with polymers **P1** and **P2**, they gave an E_a of 36 kcal/mol and 38 kcal/mol respectively as shown in Table 4.1. The structures of **P1** and **P2** are almost identical. However, between them, there is a small difference in functional spacer between the phenyl rings. The hexafluoro spacer of **P1** ($C(CF_3)_2$) does not have the slight increase in proximity and electron density of the phenyl rings as **P2** with no substituent or functional group between rings. This small increase is a likely theory as to the difference. Table **4.1** (Obtained Activation Energy)

Table 4.1 Table of Activation Energy (E_a) obtained from average rates of degradation for the studied polymers.

Polymers	Activation Energy (E_a) (kcal/mol)
P1 (PFCB-6F)	36
P2 (PFCB-BP)	38
P3 (PFCA)	20
P4 (FAVE-Acenaphthenone)	25
P5 (FAVE-Phenanthrenone)	17
P6 (Thermoset)	20
P6 (Glassy Carbon)	41

The next few energies belong to **P3** (20 kcal/mol), **P4** (25 kcal/mol) and **P5** (17 kcal/mol). These polymers have fluorinated aryl vinyl ether (FAVE) linkages between monomers. The notable property of FAVE polymers is their ability for chain propagation due to reactive TFVE end groups to further grow the chain or undergo polymerization into PFCB rings. This crucial property is the likely reason for the lower activation energies in reference to the other polymers. **P3** is very similar to **P4** in which it has a perfluorocyclohexyl aromatic (PFCA) ring substituted spacer but same core structure. Perfluorocyclohexyl aromatic ether polymers are also known for their stability along with FAVEs and PFCBs. The increased ring size between **P4** and **P5** and electron density may account for the difference between them. **P5** is the lowest with 17 kcal/mol and has a difference in a core cyclohexane ring versus a core pentane ring compared to **P4** that may decrease conjugation and electron density over the structure leading to a decrease in stability. **P6** or bis-*o*-diynyl aryl ether (BODA-Ether) is a known polymer that has been reported to have high thermostability and minuscule weight loss until <1%/h at 450 °C[28]. Its activation energy was obtained in its thermoset state (>450°C) and later as a cured glassy carbon (>900°C). Due to the novel properties of BODA derivatives having phenyl substituted monomers, they can yield highly crosslinked polynapthalene networks of superior thermal

resistance leading to the highest activation energy on the table[28]. The BODA-Ether thermoset of **P6** was unexpectedly low, 20 kcal/mol, and was among the level of FAVE polymers. The polymer itself may not have been fully cured to the polynapthalene network during the heating process.
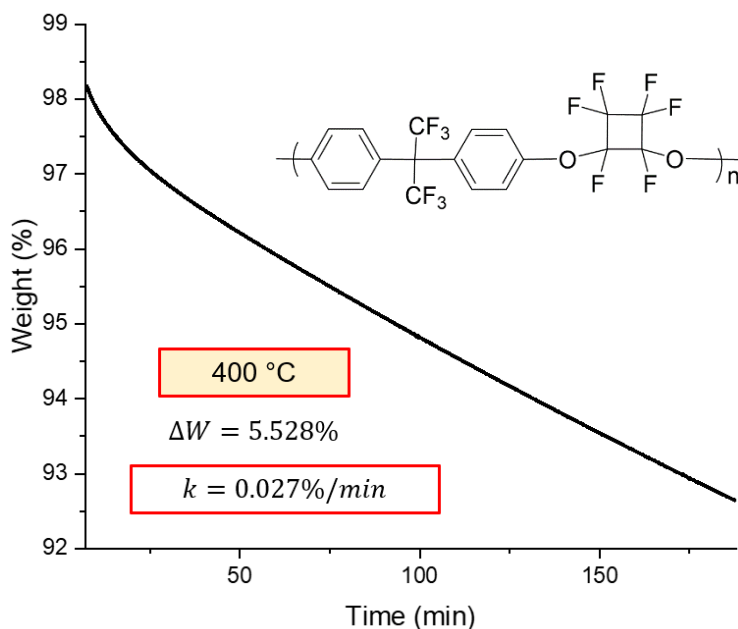

Figure 4.5 Isothermal TGA of PFCB-6F

An isothermal TGA spectra of PFCB-6F at 400 over a 3-hr. time interval in which weight loss and rate of weight loss can be obtained.

The energies obtained so far are based on the average rate of degradation per/h over the 3-hour isothermal experiment. It is of interest to gauge the specific rate of degradation during the interval closet to zero ordered behavior as possible. Isothermal TGA spectra for the selected polymers can be found in Appendix **A.3**. The rates of the middle 60 min interval were obtained in %/min that were then converted to %/h (Figure **4.5**). The Arrhenius plots for these spectra were graphed for each of the selected polymers (Figure **4.6**) The middle interval was used in case artifacts from the TGA instrument caused any abnormalities in the first 60 min interval of the experiment. The area in which the rate is obtained can also affect the trend of activation energies

33

obtained from the polymers. The new rates yielded energies of varying difference compared to the previous table. The new energies are closer to actual values observed from the degradation of the selected polymers as shown in Table **4.2**. Some of the polymers did not change at all like **P1** and **P2** while others like **P3** and **P4** changed a great deal. **P5** and **P6** changed only slightly with the new obtained energies. The Glassy Carbon of **P6** decreased in likely part due to the instrument not having the capabilities to go completely to the glassy carbon.
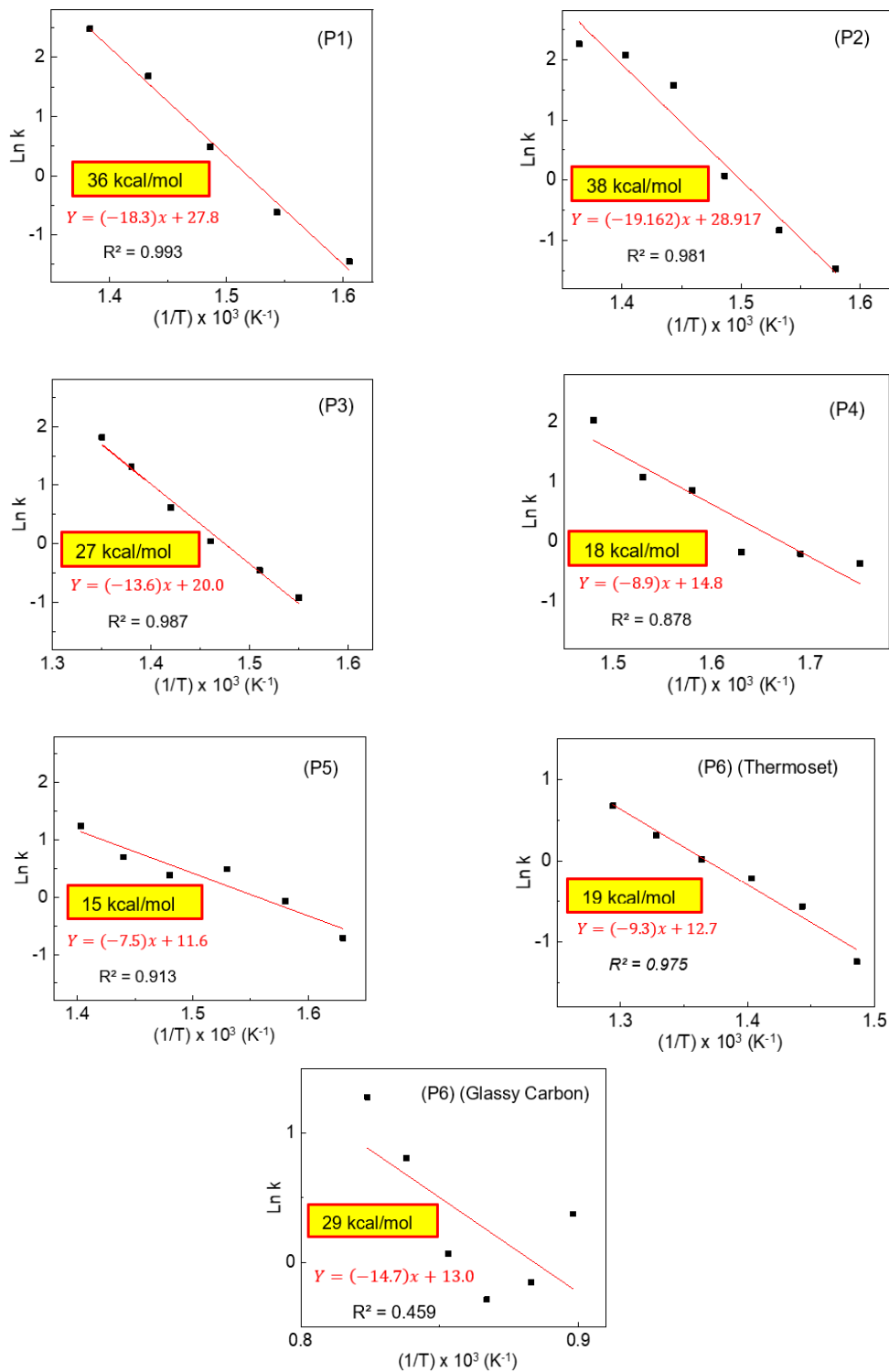
Figure 4.6 (Arrhenius Plots based on a specific rate)

Arrhenius plots for the selected polymers based on the middle 60 min interval of the isothermal experiment.

Table 4.2 Table of Activation Energy (E_a) obtained from the average degradation rate over 3 hrs versus the middle 60 min interval.

Polymers	Activation Energy (E_a) (kcal/mol)	
	Avg	Mid 60
P1 (PFCB-6F)	36	36
P2 (PFCB-BP)	38	38
P3 (PFCA)	20	27
P4 (FAVE-Acenaphthenone)	25	18
P5 (FAVE-Phenanthrenone)	17	15
P6 (Thermoset)	20	19
P6 (Glassy Carbon)	41	29

Another variable affecting the activation energy difference is the mechanism for how polymers degrade over time. The science behind the theory of fluoropolymer decomposition has been reported since in the 1950's[27]. **P1** – **P5** contain fluorinated linkages. The method of decomposition is relatively simple as reported in 1990s from the literature on PFCB decomposition[22]. For PFCB polymers, as it is heated to high temperatures, there are some by products blown off but one of the main products is a hexafluorocylcobutene ring. As polymers are heated, known products like CO_2 and H_2O are produced so BDE energies matter. The BDE of simple sigma bonds like C-C and C-O take ~ 350 kJ/mol to break so a possible C-O bond may be susceptible to breakage at high temperatures before C-H bonds or C-F bonds of ~ 413 kJ/mol and ~ 472 kJ/mol BDE. The ring results from homolytic cleavage of both of the oxygen bonds connected to the ring, releasing hexafluorocyclobutene. Because of the high temperature environment, it was just released into, the hexafluorocyclobutene ring may ring open to hexafluoro-1,3-butadiene. This type of ring opening is an electrocyclic reaction. These reversible reactions have single bonds form at the terminal ends of the pi bond. The driving force for this reaction can be attributed it to ring strain of the cyclobutene ring[8]. The free electrons around

36

fluorine are highly polar and cause strain on the ring and force the structure to achieve a more favorable confirmation with less strain[8]. There is a similar theory to the decomposition of FAVEs at high temperatures. The fluorinated vinyl spacer between monomers could revert into a fluorinated acetylene upon homolytic breakage as it degrades. This is similar mechanism to the degradation of PFCBs. A proposed mechanism of degradation is shown in Scheme **4.1.**
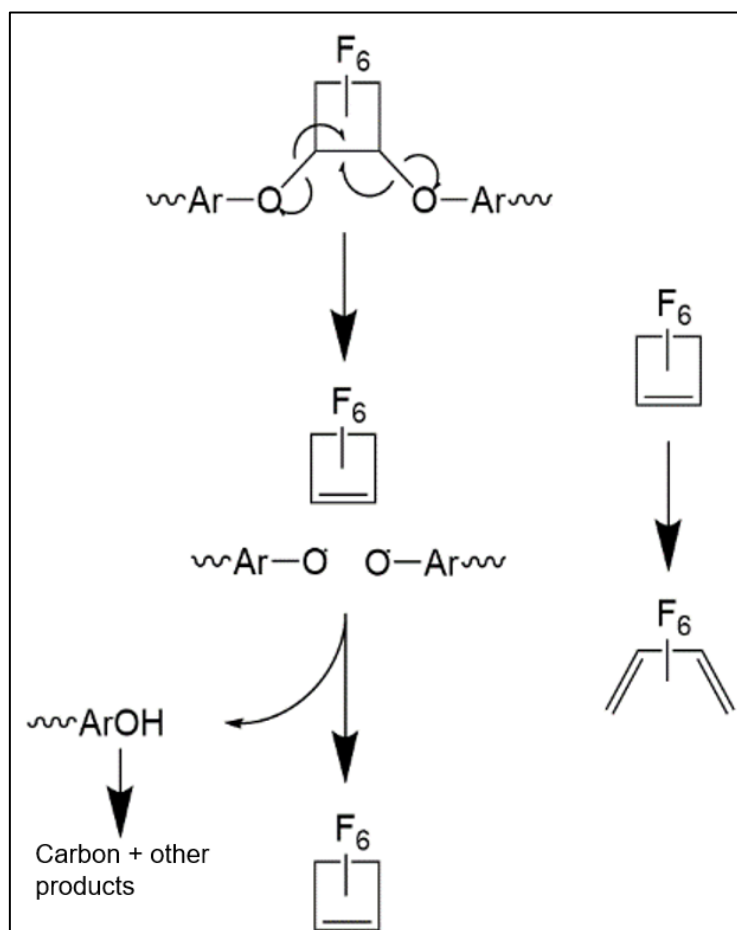
Scheme 4.1 Proposed Degradation Mechanism

Proposed mechanism for the degradation of perfluorocyclobutyl aryl ether polymers.

The main attribute differentiating the polymers from one another in terms of activation energy is chemical structure as well as the behavior of the intramolecular and intermolecular interactions along and between the polymer chains. So, the choice for foundation of TFVE oligomers is critical to the degree of mechanical and chemical properties desired. The changes in core structure or substituents attached can be seen in the behavior of the Arrhenius plots and obtained activation energies. The activation energy of each polymer is obtained and an Arrhenius plot for depiction of the rate kinetics.

Zero ordered rates are independent of concentration and only depend on the rate itself in controlled conditions. TGA methods using zero-ordered parameters can be used to thoroughly investigate the structure of the polymer under study. TGA is used to observe the rate of weight loss of a sample as it is heated in an isolated space of known atmosphere for a pre-set time interval. The weight loss calculated from these experiments are readily given as thermal stability parameters for a number of polymers. Quantitatively we can estimate weight loss from internal reactions or byproducts throughout the reaction in the known atmosphere but we do not know exactly what those reactions are. We can speculate what is going on based on the starting sample and the resulting char at the end of the TGA run. However, TGA alone cannot tell us what specifically is happening to the sample at the selected temperature. There is a need to change our perspective on thermal stability like technology has with time.

The obtained activation energies of the polymers give us more insight into the thermal parameters of these polymers. The notion is that thermal stability or thermal resistance as they are often confused are the same but there is doubt. Thermal stability has been perceived as the resistance of a polymer to a heat source. I believe this notion needs to be changed and our theory

38

of thermal stability with it. Thermal stability should be more perceived as resistance of a polymer to the environment induced by heat. Heat can make environments and materials hot but it can also cause bonds to break and form as well as react in general. If a polymer could resist the environment that comes with increased heat, then it could be considered thermally stable.

4.2 Polymer Conversion by Raman

Raman spectroscopy was used in this work in order to fully characterize, for the first time, a well-known polymer for applications in engineering and mechanics. Some polymers of high molecular weight or with certain properties make it difficult to characterize them. The use of Raman can save time and give information not accessible using other techniques for the same purpose. Raman spectroscopy was done on crosslinked BODA-biphenyl and carbon fiber at different cure states in order to follow it by Raman and notice any distinct differences that could give us an idea of the morphology and changes to it at higher temperatures (Figure **4.7**). Raman was taken at different intervals of the carbonization process. A standard carbon fiber for comparison was also shown in reference. BODA-biphenyl monomer is given at the bottom. The crosslinked composite state at 1000 °C and 1500 °C were taken respectively. The same was done with the carbon fiber standard and it was heated to glassy carbon (1000 °C). BODA-biphenyl monomer was crosslinked with carbon fibers and heated from monomer state to fully carbonized glassy carbon composite state. A Raman spectrum of the BODA thermoset was unable to be obtained. The state of the BODA polymer in this state is highly fluorescent as it is further cured into glassy carbon as it adopts more a polynapthalene network and many bonds are breaking and forming simultaneously. The heightened fluorescence pollutes the spectra and overshadows any other potential peaks for characterization. Two noticeable peaks around 1580 cm^{-1} and 1360

39

cm^{-1} are the most prominent on the spectra for identifying and characterizing P6's structure.

The peak at ~1580 cm^{-1} is representative of (-C=C-) bond stretching and vibrational modes of

sp² atoms constituting the chains and polycyclic rings. The peak at 1360 cm^{-1} is representative

of similar (-C=C-) vibrations. However, this peak is synonymous with a cluster of sp² hybridized

clusters that are midway through the conversion process. This entails that the current spectra are

of the sample at a state not fully carbonized.
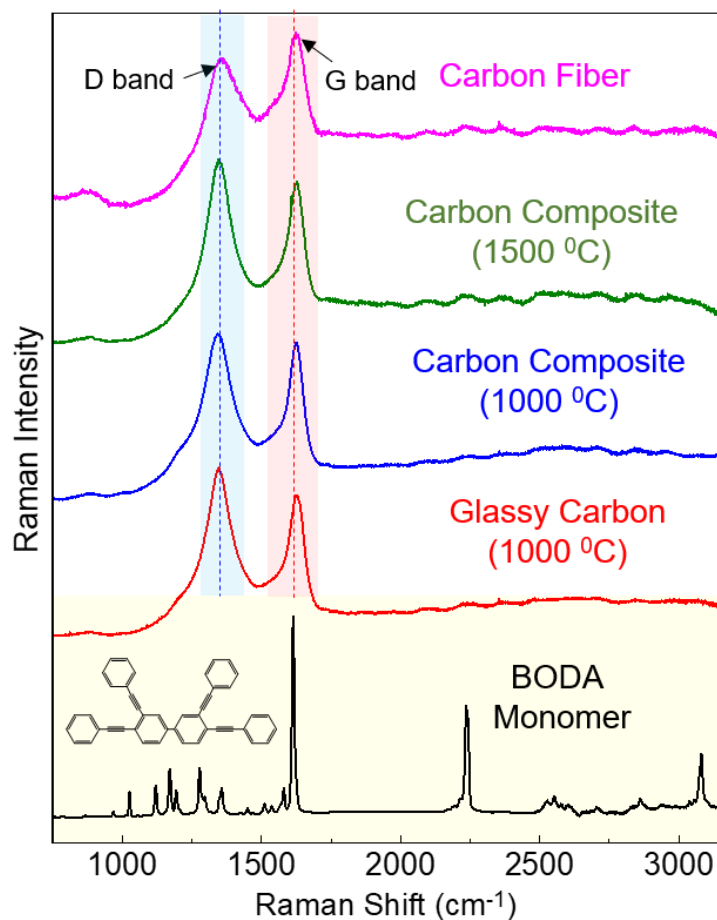
Figure 4.7 Raman overlay spectra

Ramen overlay spectra of polymer conversion of BODA monomer, crosslinked BODA
composite and carbon fiber standard.

BODA-Biphenyl has been reported and characterized but not through the use of Raman Spectroscopy. BODA-Biphenyl starts to resemble a graphitic like morphology when it polymerizes into its naphthalene network thermoset and further as a glassy carbon composite. The peak at ~1600 cm^{-1} ,which is an indicator of aromatic (C=C) chain vibrations, is in the BODA sample as well as the carbon fiber matrix. The other peak at ~1320 cm^{-1} is also seen in both samples. These two peaks are known as the "G" band (~1580 cm^{-1}) and "D" band (~1360 cm^{-1}) respectively[25]. The "G" band is named so because it is the main peak associated with graphene structures and is named "G" for graphene because of that. The "D" band is associated with disorder. The higher the "D" peak the more disorder inside the polymer matrix. This disorder is a cluster of hybridized sp² carbons that have not fully carbonized. The height and concentration of the peak directly relate to the carbonization conversion of the sample. Using these two peaks in conjunction, we identify the BODA sample as having graphene like morphology and good indication of crosslinked product between the BODA-Biphenyl and carbon fiber.

The Raman spectra obtained are similar to reported evidence of high similarity to the graphene network. BODA-Biphenyl starts to adapt to the graphene-like morphology after polymerizing at ~ 450 °C so Raman was taken of samples past this temperature. The obtained spectra shows that it is possible to follow the polymer network as it cures and forms more stacked sheets on top of itself. There is also similarity between the crosslinked product and the standard carbon fiber. Bis-o-diynylarene (BODA) derivatives are well known for their high thermal stability and mechanical properties. These properties can be coupled with carbon fibers to produce a new high-performance polymer for material science. This spectrum has incredible

potential for future application as other derivatives of BODA and other known high-performance

polymers can be characterized and followed by Raman spectroscopy.

CHAPTER V

CONCLUSION

This study reports an established method using TGA and 0th order kinetics to study the thermal stability of six aromatic ether polymers, five of which were semi-fluorinated. Activation energies for thermal degradation ranging from 17 (kcal/mol) to 41 (kcal/mol) were also reported here. The difference in overall structure and degradation mechanism played a factor in the trend of the activation energies. **P6** (BODA-Ether) glassy carbon had the highest E_a of 41 kcal/mol. The next two were the PFCB based polymers (**P1** and **P2**) with 36 kcal/mol and 38 kcal/mol. Lastly were the FAVE and PFCA polymers (**P3** – **P5**) with 17, 20, and 25 kcal/mol. The trend of activation energies was expected. The reaction energy difference of ~ 50 kcal/mol favoring the forward reaction versus the reverse reaction for PFCB ring formation of fluoro-olefins also helps support how thermally stable PFCB polymers are. The degradation mechanism also played a role in differences between the semi-fluorinated polymers. PFCBs tend to form hexafluorocyclobutene rings upon degradation after homolytic bond breaking between oxygen and the PFCB ring. FAVEs release a fluoroacetylene molecule after decomposition. The difference in decomposition mechanism affects the overall stability of the polymer. The Arrhenius plots of the fluorinated polymers showed similar behavior between similar polymers to characterize and distinguish them into PFCB or FAVE. The BODA-Ether, being primarily made of carbons and hydrogens, resembled graphitic material and was the most thermally stable according to the table of activation energies. Raman studies were also performed on BODA-

43

biphenyl to characterize the known polymer and chart its similarity to graphitic structures. Noticeable peaks at 1600 cm^{-1} and 1320 cm^{-1} represent the "G" and "D" band of graphene respectively. This leads to more in-depth studies into the characterization and optical applications for high performance alongside carbon fiber. The ultimate gain of this study was to establish a protocol for studying thermal stability through 0th order kinetics. Through the use of this technique, we can better understand the slight changes to structure that can affect the rate of decomposition and activation energy of the selected polymer.

REFERENCES

[1] Friedrich, K. (2018). Polymer composites for tribological applications. *Advanced Industrial and Engineering Polymer Research, 1*(1), 3-39. doi:https://doi.org/10.1016/j.aiepr.2018.05.001

[2] Rose, J. B. (1974). Preparation and properties of poly(arylene ether sulphones). *Polymer, 15*, 456-465.

[3] Lauzon, M. (2012). Diversified Plastics Inc., PEEK playing role in space probe. *Crain Communications Inc.* Retrieved from plasticnews.com

[4] Rosof, B. H. (1989). The metal injection molding process comes of age. *JOM Journal of the Minerals Metals and Materials Society, 41*(8), 13-16. doi:10.1007/BF03220295

[5] Zeus Industrial Products, I. (2019). Understanding Fluoropolymers. *AZoM*. Retrieved from https://www.azom.com/article.aspx?ArticleID=17673

[6] Teng, H. (2012). Overview of the Development of the Fluoropolymer Industry. *Applied Sciences, 2*, 496-512. doi:10.3390/app2020496

[7] Babb, D. A., Ezzell, B. R., Clement, K. S., Richey, W. F., & Kennedy, A. P. (1993). Perfluorocyclobutane aromatic ether polymers. *Journal of Polymer Science Part A: Polymer Chemistry, 31*(13), 3465-3477. doi:10.1002/pola.1993.080311336

[8] Smith, D. W., & Babb, D. A. (1996). Perfluorocyclobutane Aromatic Ether Polymers. II. Thermal/Oxidative Stability and Decomposition of a Thermoset Polymer. *Macromolecules, 29*(3), 852-860. doi:10.1021/ma951149b.

[9] Smith Jr., D. W., Babb, D. A., Shah, H. V., Hoeglund, A., Traiphol, R., Perahia, D., . . . Radler, M. (2000). Perfluorocyclobutane (PFCB) polyaryl ethers: versatile coatings materials. *Journal of Fluorine Chemistry, 104*(1), 109-117. doi:https://doi.org/10.1016/S0022-1139(00)00233-5

[10] Lewis, E. E., & Naylor, M. A. (1947). Pyrolysis of Polytetrafluoroethylene. *Journal of the American Chemical Society, 69*(8), 1968-1970. doi:10.1021/ja01200a039

[11] Bernett, W. A. (1969). Hybridization effects in fluorocarbons. *The Journal of Organic Chemistry, 34*(6), 1772-1776. doi:10.1021/jo01258a054

[12] Iacono, S. T. (2008). Semifluorinated Polymers via Cycloaddition and Nucleophilic Addition Reactions of Aromatic Trifluorovinyl Ethers. *Ph. D Thesis, Clemson University*.

[13] Lacher, J. R., Tompkin, G. W., & Park, J. D. (1952). The Kinetics of the Vapor Phase Dimerization of Tetrafluoroethylene and Trifluorochloroethylene1. *Journal of the American Chemical Society, 74*(7), 1693-1696. doi:10.1021/ja01127a024

[14] Madorsky, S. I. H., V.E.; Straus, S.; Sedlak, V.A. (1953). Thermal Degradation of tetrafluoroethylene and hydrofluoroethylene polymers in a vacuum. *National Bureau of Standards, 51*(6), 327.

[16] Beckerbauer, R. (1968). Fluorocarbon ethers. U.S. Patent 3,397,191.

[17] Iacono, S. T., Budy, S. M., Jin, J., & Smith Jr., D. W. (2007). Science and technology of perfluorocyclobutyl aryl ether polymers. *Journal of Polymer Science Part A: Polymer Chemistry, 45*(24), 5705-5721. doi:10.1002/pola.22390.

[18] Kettwich, S. C., Lund, B. R., Smith, D. W., & Iacono, S. T. (2012). Recent Advances in Partially Fluorinated Arylene Vinylene Ether (FAVE) Polymers. In *Advances in Fluorine-Containing Polymers* (Vol. 1106, pp. 9-28): American Chemical Society

[19] Iacono, S. T., Budy, S. M., Ewald, D., & Smith Jr., D. W. (2006). Facile preparation of fluorovinylene aryl ether telechelic polymers with dual functionality for thermal chain extension and tandem crosslinking. *Chemical Communications*(46), 4844-4846. doi:10.1039/B610157G

[20] Flynn, J. H., & Wall, L. A. (1966). A quick, direct method for the determination of activation energy from thermogravimetric data. *Journal of Polymer Science Part B: Polymer Letters, 4*(5), 323-328. doi:https://doi.org/10.1002/pol.1966.110040504

[21] Sørensen, O. T. (1978). Thermogravimetric studies of non-stoichiometric cerium oxides under isothermal and quasi-isothermal conditions. *Journal of Thermal Analysis and Calorimetry, 13*(3), 429. doi:10.1007/bf01912383

[22] Babb, D. A., Boone, H. W., Smith Jr, D. W., & Rudolf, P. W. (1998). Perfluorocyclobutane aromatic ether polymers. III. Synthesis and thermal stability of a thermoset polymer containing triphenylphosphine oxide. *Journal of Applied Polymer Science, 69*(10), 2005-2012. doi:10.1002/(SICI)1097-4628(19980906)69:10<2005::AID-APP12>3.0.CO;2-0

[23] Ferrari, A. C. (2007). Raman spectroscopy of graphene and graphite: Disorder, electron–phonon coupling, doping and nonadiabatic effects. *Solid State Communications, 143*(1), 47-57. doi:https://doi.org/10.1016/j.ssc.2007.03.052

[24] Okuda, H., Young, R. J., Wolverson, D., Tanaka, F., Yamamoto, G., & Okabe, T. (2018). Investigating nanostructures in carbon fibres using Raman spectroscopy. *Carbon, 130*, 178-184. doi:https://doi.org/10.1016/j.carbon.2017.12.108

[25] Childres, I., Jauregui, L., Park, W., Caoa, H., & Chena, Y. P. (2013). Raman Spectroscopy of Graphene and Related Materials. *New Developments in Photon and Materials Research*, 403-418.

[26] Athukorale, S., Perera, G. S., Gadogbe, M., Perez, F., & Zhang, D. (2017). Reactive Ag+ Adsorption onto Gold. *The Journal of Physical Chemistry C, 121*(40), 22487-22495. doi:10.1021/acs.jpcc.7b07077

[27] Atkinson, B., & Trenwith, A. B. (1953). 424. The thermal decomposition of tetrafluorethylene. *Journal of the Chemical Society (Resumed)*(0), 2082-2087. doi:10.1039/JR9530002082

[28] Shah, H. V., Brittain, S. T., Huang, Q., Hwu, S. J., Whitesides, G. M., & Smith Jr., D. W. (1999). Bis-o-diynylarene (BODA) Derived Polynaphthalenes as Precursors to Glassy Carbon Microstructures. *Chemistry of Materials, 11*(10), 2623-2625. doi:10.1021/cm9903780

[29] Wlassics, I. (2004). $2\pi + 2\pi$ cycloaddition kinetics of some fluoro olefins and fluoro vinyl ethers. *Journal of Fluorine Chemistry - J FLUORINE CHEM, 125*, 1519-1528. doi:10.1016/j.jfluchem.2004.06.014

[30] Smith Jr., D. W., Jin, J., Shah, H. V., Xie, Y., & DesMarteau, D. D. (2004). Anomalous crystallinity in a semi-fluorinated perfluorocyclobutyl (PFCB) polymer containing the hexafluoro-i-propylidene (6F) linkage. *Polymer, 45*(17), 5755-5760. doi:https://doi.org/10.1016/j.polymer.2004.06.011

[31] Park, J. (2013). Sulfonated Perfluorocyclobutyl (PFCB) Aryl Ether Polymers: Synthesis, Reactivity, and Characterization for Polymer Electrolyte Applications. *Ph.D Thesis, Clemson University*

[32] Stuart, B. H. (1996). Polymer crystallinity studied using Raman spectroscopy. *Vibrational Spectroscopy, 10*(2), 79-87. doi:https://doi.org/10.1016/0924-2031(95)00042-9

[33] Cheatham, C. M., Lee, S. N., Laane, J., Babb, D. A., & Smith, D. W. (1998). Kinetics of trifluorovinyl ether cyclopolymerization via Raman spectroscopy. *Polymer International, 46*(4), 320-324.

[34] Hodkiewicz, J. (2010). *Characterizing Carbon Materials with Raman Spectroscopy*.

[35] Nielsen, A. S., Batchelder, D. N., & Pyrz, R. (2002). Estimation of crystallinity of isotactic polypropylene using Raman spectroscopy. *Polymer, 43*(9), 2671-2676. doi:https://doi.org/10.1016/S0032-3861(02)00053-8

[36] Parnell, S., Min, K., & Cakmak, M. (2003). Kinetic studies of polyurethane polymerization with Raman spectroscopy. *Polymer, 44*(18), 5137-5144. doi:https://doi.org/10.1016/S0032-3861(03)00468-3

[37] Farajidizaji, B., Shelar, K. E., Narayanan, G., Mukeba, K. M., Donnadieu, B., Pittman Jr, C. U., Smith Jr, D. W. (2019). Acenaphthylene-derived perfluorocyclobutyl aromatic ether polymers. *Journal of Polymer Science Part A: Polymer Chemistry, 57*(12), 1270-1274. doi:10.1002/pola.29388

[38] Perera, K. P., Abboud Ka Fau - Smith Jr., D. W., Fau - Krawiec, M., & Krawiec, M. Three bis-ortho-diynylarenes (BODA). (0108-2701 (Print)).

[39] Améduri, B. (2020). The Promising Future of Fluoropolymers. *Macromolecular Chemistry and Physics, 221*(8), 1900573. doi:10.1002/macp.201900573

[40] B. Farajidizaji, K. E. Shelar, G. Narayanan, K. M. Mukeba, B. Donnadieu, C. U. Pittman Jr, A. Sygula and D. W. Smith Jr, *Journal of Polymer Science Part A: Polymer Chemistry* **2019**, *57*, 1270-1274.

[41] Wang, Y., Wang, J., Jin, K., Sun, J., & Fang, Q. (2016). A new glass-forming molecule having a fluorene skeleton: synthesis and conversion to the polymer with a low dielectric constant, high hydrophobicity and thermostability. *Polymer Chemistry, 7*(38), 5925-5929. doi:10.1039/C6PY01212D

[42] Wang, J., Li, K., Yuan, C., Jin, K., Tian, S., Sun, J., & Fang, Q. (2015). Variable Polymer Properties Driven by Substituent Groups: Investigation on a Trifluorovinylether-Functionalized Polyfluorene at the C-9 Position. *Macromolecular Chemistry and Physics, 216*(7), 742-748. doi:10.1002/macp.201400597

[43] Dei, D. K., Lund, B. R., Wu, J., Simon, D., Ware, T., Voit, W. E., . . . Smith, D. W. (2013). High Performance and Multipurpose Triarylamine-Enchained Semifluorinated Polymers. *ACS Macro Letters, 2*(1), 35-39. doi:10.1021/mz300532z

[44] Shinzawa, H., Ozaki, Y., & Chung, H. (2012). Study of the pre-melting behavior of polyethylene using Raman spectroscopy combined with two-dimensional (2D) correlation spectroscopy. *Vibrational Spectroscopy, 60*, 154-157. doi:https://doi.org/10.1016/j.vibspec.2011.11.007

[45] P Ptáček, P., Kubátová, D., Havlica, J., Brandštetr, J., Šoukal, F., & Opravil, T. (2010). Isothermal kinetic analysis of the thermal decomposition of kaolinite: The thermogravimetric study. *Thermochimica Acta, 501*(1), 24-29. doi:https://doi.org/10.1016/j.tca.2009.12.018

[46] Iacono, S. T., Budy, S. M., Mabry, J. M., & Smith, D. W. (2007b). Synthesis, Characterization, and Surface Morphology of Pendant Polyhedral Oligomeric Silsesquioxane Perfluorocyclobutyl Aryl Ether Copolymers. *Macromolecules, 40*(26), 9517-9522. doi:10.1021/ma071732f

[47] Iacono, S. T., Budy, S. M., Mabry, J. M., & Smith, D. W. (2007a). Synthesis, characterization, and properties of chain terminated polyhedral oligomeric silsesquioxane-functionalized perfluorocyclobutyl aryl ether copolymers. *Polymer, 48*(16), 4637-4645. doi:https://doi.org/10.1016/j.polymer.2007.06.022

[48] Conrad, M. P. C., & Shoichet, M. S. (2007). Synthesis and thermal stability of hybrid fluorosilicone polymers. *Polymer, 48*(18), 5233-5240. doi:https://doi.org/10.1016/j.polymer.2007.07.014

[49] Spraul, B., Suresh, S., Glaser, S., Perahia, D., Ballato, J., & Smith, D. (2004). Perfluorocyclobutyl-Linked Hexa- p eri -hexabenzocoronene Networks. *Journal of the American Chemical Society, 126*, 12772-12773. doi:10.1021/ja046855j

[50] Huang, X., Wang, R., Zhao, P., Lu, G., Zhang, S., & Qing, F.-l. (2005). Synthesis and characterization of novel fluoropolymers containing sulfonyl and perfluorocyclobutyl units. *Polymer, 46*(18), 7590-7597. doi:https://doi.org/10.1016/j.polymer.2005.06.016

[51] Smith Jr, D. W., Chen, S., Kumar, S. M., Ballato, J., Topping, C., Shah, H. V., & Foulger, S. H. (2002). Perfluorocyclobutyl Copolymers for Microphotonics. *Advanced Materials, 14*(21), 1585-1589. doi:10.1002/1521-4095(20021104)14:21<1585::AID-ADMA1585>3.0.CO;2-S

[52] Smith Jr., D. W., Hoeglund, A. B., Shah, H. V., Radler, M. J., & Langhoff, C. A. (2001). Perfluorocyclobutane Polymers for Optical Fiber and Dielectric Waveguides. In *Optical Polymers* (Vol. 795, pp. 49-62): American Chemical Society

[53] Persenaire, O., Alexandre, M., Degée, P., & Dubois, P. (2001). Mechanisms and Kinetics of Thermal Degradation of Poly(ε-caprolactone). *Biomacromolecules, 2*(1), 288-294. doi:10.1021/bm0056310.

[54] O. Persenaire, M. Alexandre, P. Degée and P. Dubois, *Biomacromolecules* **2001**, *2*, 288-294.

[55] Harmon, J. (2001). Polymers for Optical Fibers and Waveguides: An Overview. In (Vol. 795, pp. 1-23).

[56] Salin, I. M., & Seferis, J. C. (1993). Kinetic analysis of high-resolution TGA variable heating rate data. *Journal of Applied Polymer Science, 47*(5), 847-856. doi:10.1002/app.1993.070470512

[57] Duus, H. C. (1955). Thermochemical Studies on Fluorocarbons - Heat of Formation of CF4, C2F4, C3F6, C2F4 Dimer, and C2F4 Polymer. *Industrial & Engineering Chemistry, 47*(7), 1445-1449. doi:10.1021/ie50547a051

[58] Prober, M. (1953). The Synthesis and Polymerization of Some Fluorinated Styrenes1. *Journal of the American Chemical Society, 75*(4), 968-973. doi:10.1021/ja01100a058

[59] Murrary, E. W. (1962). Polyimides or polyesterimides. *U.S. Patent* 3179634A.

[60] Zhou, J., Tao, Y., Chen, X., Chen, X., Fang, L., Wang, Y., . . . Fang, Q. (2019). Perfluorocyclobutyl-based polymers for functional materials. *Materials Chemistry Frontiers, 3*(7), 1280-1301. doi:10.1039/C9QM00001A

A.1   Dynamic TGA Plots
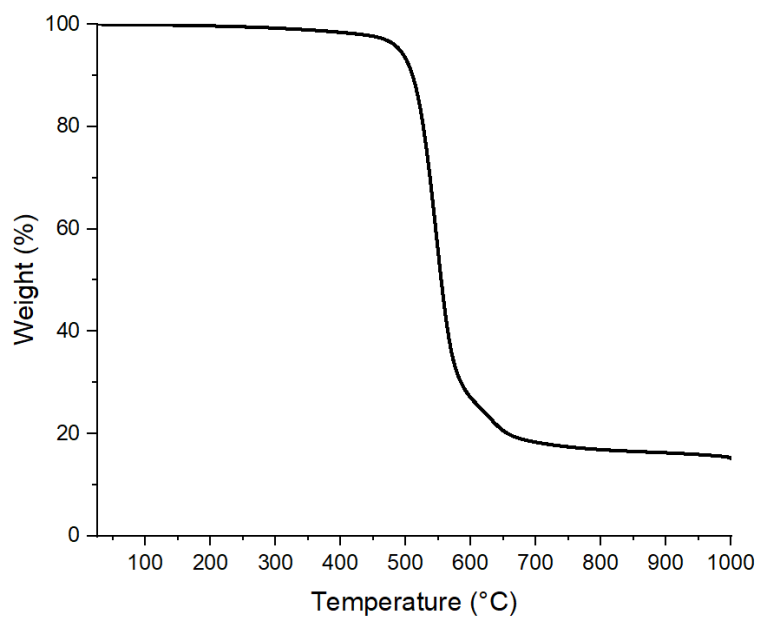
Figure A.1 (P1)

P1 heated 10 °/min from 25 °C to 1000 °C.
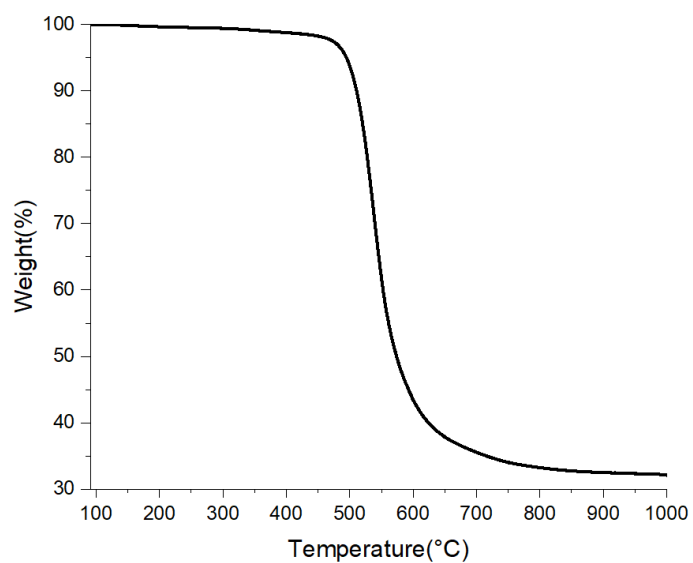
Figure A.2 (P2)

P2 heated 10 °/min from 25 °C to 1000 °C.
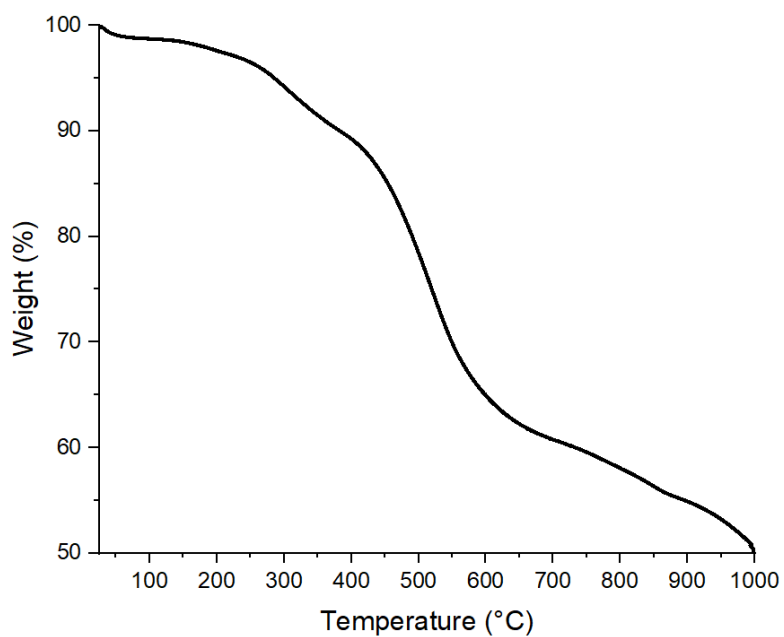
Figure A.3 (P3)

P3 heated 10 °/min from 25 °C to 1000 °C.
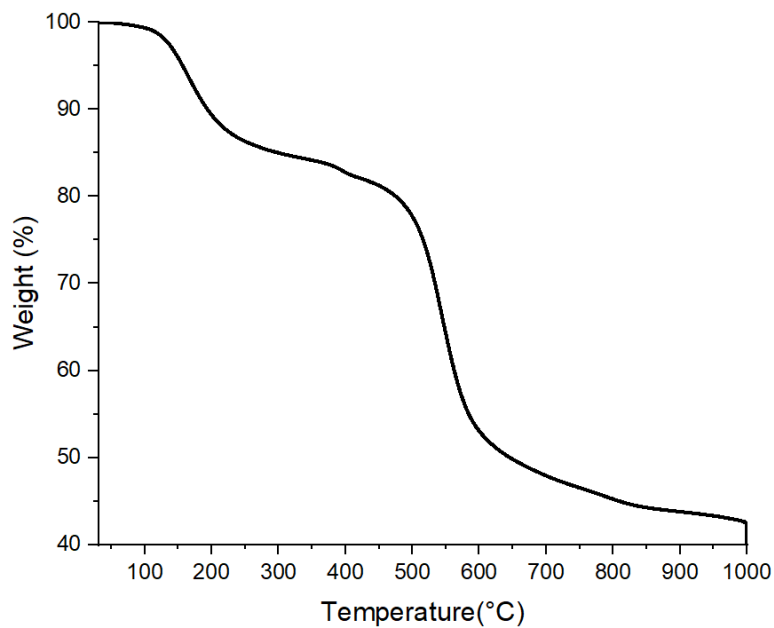
Figure A.4 (P4)

P4 heated 10 °/min from 25 °C to 1000 °C.
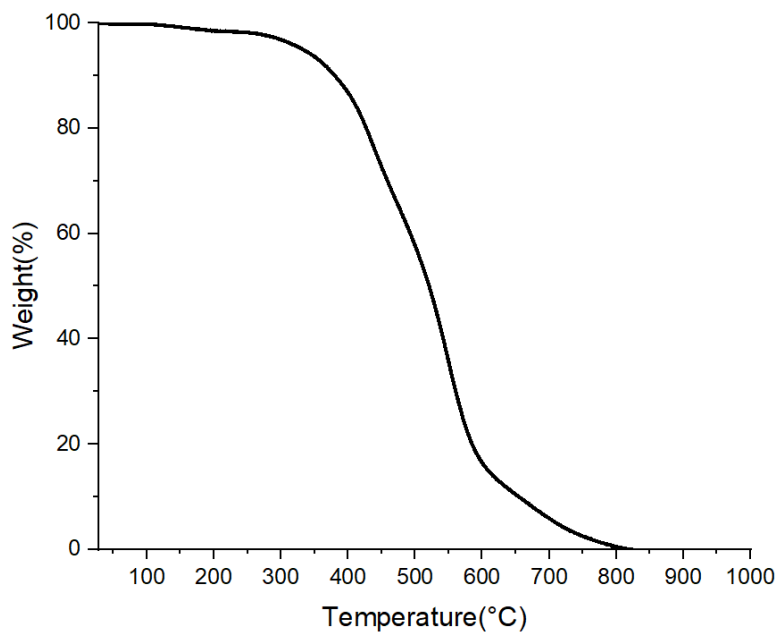
Figure A.5 (P5)

P5 heated 10 °/min from 25 °C to 1000 °C.
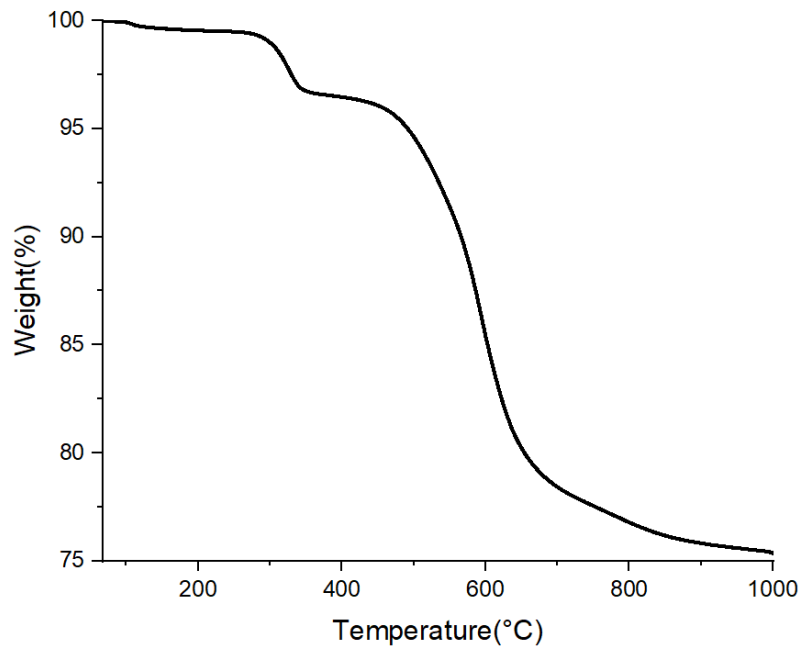
Figure A.6 (P6)

P6 heated 10 °/min from 25 °C to 1000 °C.

A.2 Parameter tables

Table A.1 Experimental parameter table of P1.

P1 Degradation Parameters

Temp. (°C)	300	325	350	375	400	425	450	475	500
Initial Wt. (mg)	16.724	14.086	9.582	10.2020	12.056	16.3130	16.5090	23.1460	11.482
Final Wt. (mg)	16.602	13.821	9.328	9.8220	11.389	13.3098	10.1233	9.5107	3.639
Wt. Change (Δ) %	0.7284	0.7241	1.130	2.084	5.528	16.60	36.29	55.99	68.30
K (%/hr.)	0.1473	0.1493	0.2461	0.5381	1.624	5.527	11.99	14.18	22.77
Ln K	-1.905	-1.902	-1.402	-0.619	0.4849	1.709	2.484	2.652	3.125
(1000)1/T(K)	1.75	1.672	1.605	1.543	1.486	1.433	1.383	1.337	1.294

Table A.2 Experimental parameter table of P2.

P2 Degradation Parameters

Temp. (°C)	340°	360°	380°	400°	420°	440°	460°	480°	500°	520°
Initial Wt. (mg)	7.952	7.831	5.530	9.491	4.748	9.648	6.493	9.841	11.153	7.354
Final Wt. (mg)	7.819	7.436	5.361	9.037	4.001	7.176	3.778	5.074	5.424	3.056
Wt. Change (Δ) %	0.6808	0.9496	1.654	3.431	14.03	23.76	40.13	46.65	48.05	48.38
K (%/hr.)	0.227	0.317	0.551	1.14	4.68	7.92	13.38	15.55	16.02	16.13
Ln K	-1.483	-1.149	-0.596	0.131	1.543	2.069	2.594	2.744	2.774	2.781
(1000)1/T(K)	1.631	1.579	1.532	1.486	1.443	1.403	1.364	1.328	1.294	1.261

Table A.3 Experimental parameter table of P3.

P3 Degradation Parameters

Temp. (°C)	370	390	410	430	450	470	490	510	530
Initial Wt. (mg)	3.09	3.11	2.50	5.23	8.67	2.62	3.25	2.29	2.56
Final Wt. (mg)	2.56	2.61	1.99	4.01	5.74	1.36	2.09	1.29	1.34
Wt. Change %	2.103	2.124	3.872	6.389	12.07	25.11	19.28	22.18	20.64
K (%/hr.)	0.701	0.708	1.29	2.13	4.02	8.38	6.43	7.39	6.88
Ln K	-0.355	-0.345	0.255	0.756	1.39	2.13	1.86	2	1.93
(1000)1/T(K)	1.55	1.51	1.46	1.42	1.38	1.35	1.31	1.28	1.25

Table A.4 Experimental parameter table of P4.

P4 Degradation Parameters

Temp. (°C)	280	300	320	340	360	380	400	420
Initial Wt. (mg)	1.89	1.87	2.23	1.50	1.41	1.29	0.391	2.26
Final Wt. (mg)	1.82	1.77	2.08	1.37	0.892	1.02	0.097	1.96
Wt. Change %	1.75	2.64	3.88	5.23	9.80	13.51	47.75	8.09
K (%/hr.)	0.582	0.878	1.29	1.74	3.27	4.50	15.9	2.69
Ln K	-0.541	-0.130	0.255	0.554	1.18	1.50	2.77	0.989
(1000)1/T(K)	1.81	1.75	1.69	1.63	1.58	1.53	1.48	1.44

Table A.5 Experimental parameter table of P5.

P5 Degradation Parameters

Temp. (•C)	300	320	340	360	380	400	420	440	460
Initial Wt. (mg)	1.09	1.89	1.88	1.44	1.53	2.12	1.74	0.996	1.49
Final Wt. (mg)	0.947	1.76	1.73	1.28	1.27	1.82	1.42	0.65	1.04
Wt. Change %	3.23	1.50	2.04	3.58	6.69	6.39	9.33	18.4	16.6
K (%/hr.)	1.08	0.50	0.68	1.19	2.23	2.13	3.11	6.13	5.53
Ln K	0.077	-0.69	-0.386	0.174	0.802	0.756	1.13	1.81	1.71
(1000)1/T(K)	1.75	1.69	1.63	1.58	1.53	1.48	1.44	1.403	1.364

Table A.6 Experimental parameter table of P6 (Thermoset).

P6 (Thermoset) Degradation parameters

Temp. (°C)	400	420	440	460	480	500	520
Initial Wt. (mg)	4.96	3.65	4.68	4.04	4.40	5.92	4.73
Final Wt. (mg)	4.91	3.57	4.53	3.91	4.18	5.67	4.22
Wt. Change %	0.916	1.98	3.25	3.21	4.95	7.89	10.76
K (%/hr.)	0.305	0.658	1.08	1.07	1.65	2.63	3.59
Ln K	-0.366	0.098	0.417	0.776	0.812	1.07	1.08
(1000)1/T(K)	1.486	1.443	1.403	1.364	1.328	1.294	1.261

Table A.7 Experimental parameter table of P6 (Glassy Carbon).

P6 (Glassy Carbon) Degradation parameters

Temp. (°C)	840	860	880	900	920	940	960	980	1000
Initial Wt. (mg)	4.60	4.99	4.49	3.83	3.56	3.56	4.68	5.79	8.35
Final Wt. (mg)	3.20	3.24	4.37	3.66	3.24	2.98	4.46	5.45	6.73
Wt. Change %	2.32	2.94	2.29	3.39	6.632	11.68	3.46	4.36	14.46
K (%/hr.)	0.772	0.979	0.765	1.13	2.21	3.89	1.15	1.45	4.82
Ln K	-0.258	-0.021	-0.267	0.122	0.793	1.36	0.141	0.374	1.57
(1000)1/T(K)	0.898	0.883	0.867	0.853	0.838	0.824	0.811	0.798	0.786

A.3   Isothermal TGA Plots

A.3.1   P1 PFCB-6F
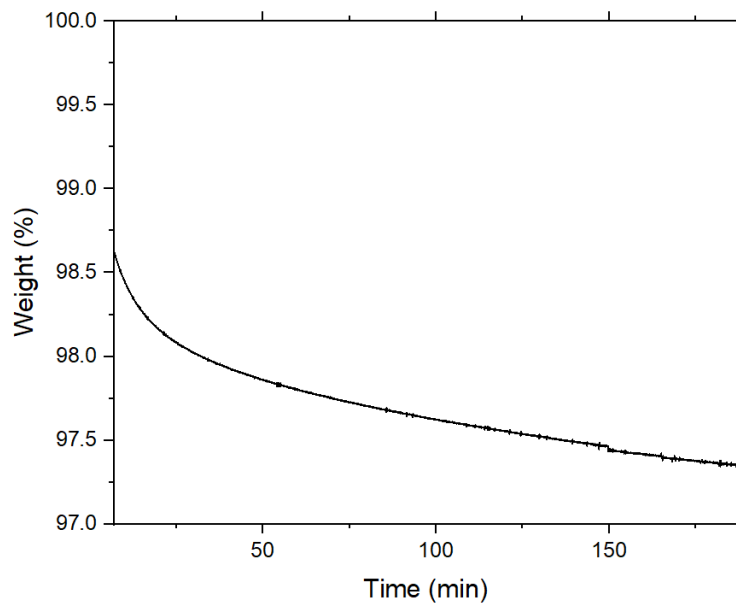
Figure A.7 (Isothermal TGA held at 350 °C)

Isothermal TGA of **P1** held at 350 °C for 3 hrs.
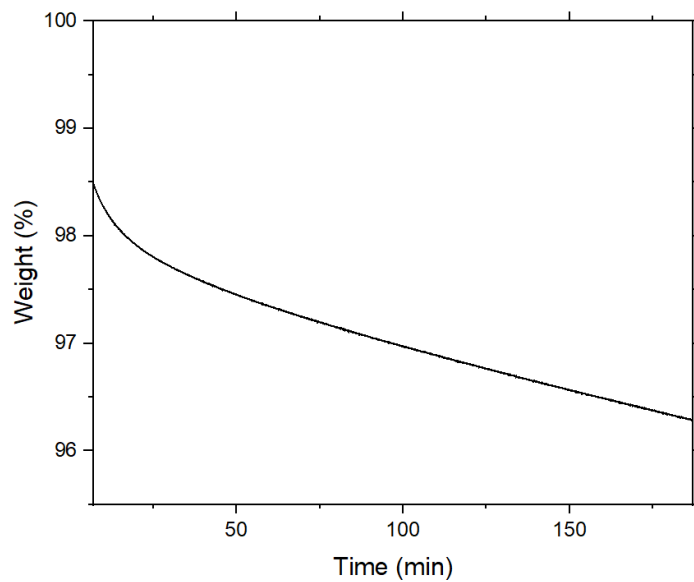
Figure A.8 (Isothermal TGA held at 375 °C)

Isothermal TGA of **P1** held at 375 °C for 3 hrs.
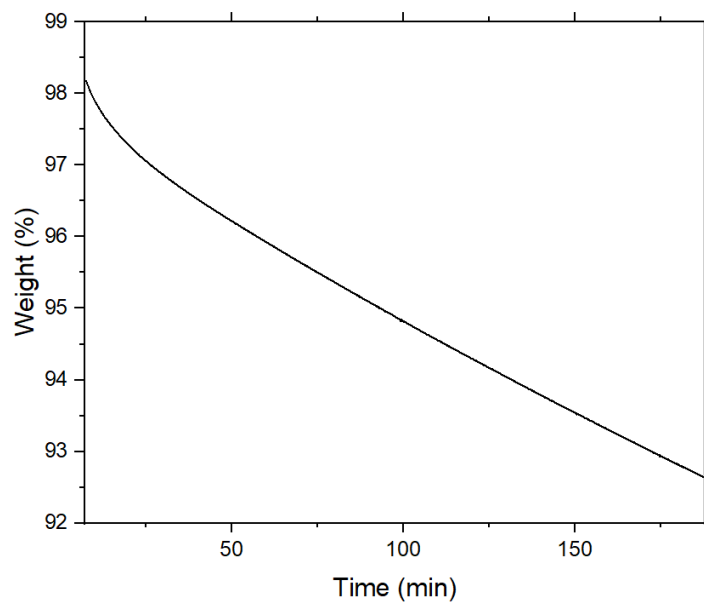
Figure A.9 (Isothermal TGA held at 400 °C)

Isothermal TGA of **P1** held at 400 °C for 3 hrs.
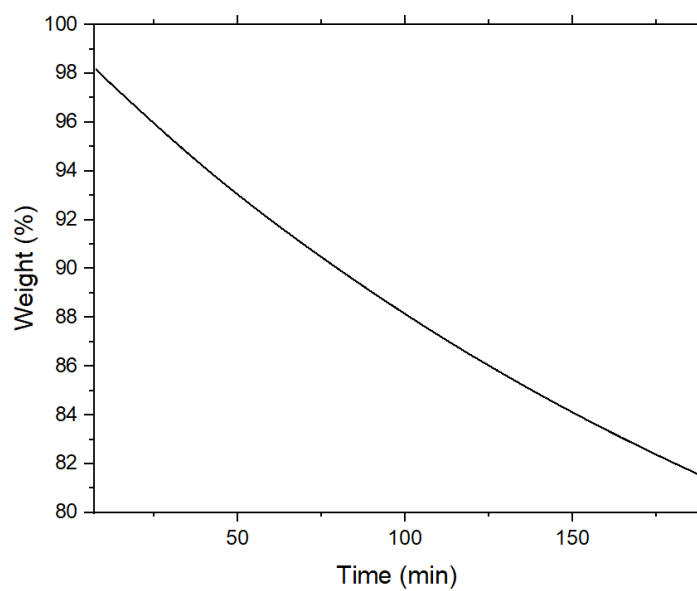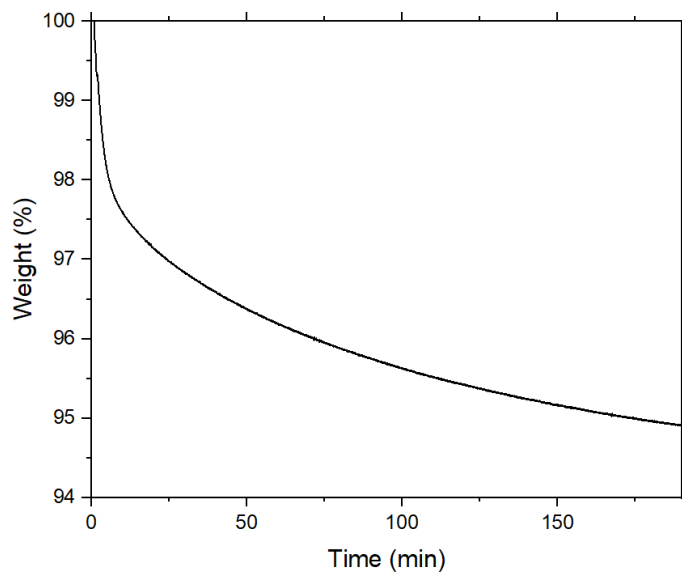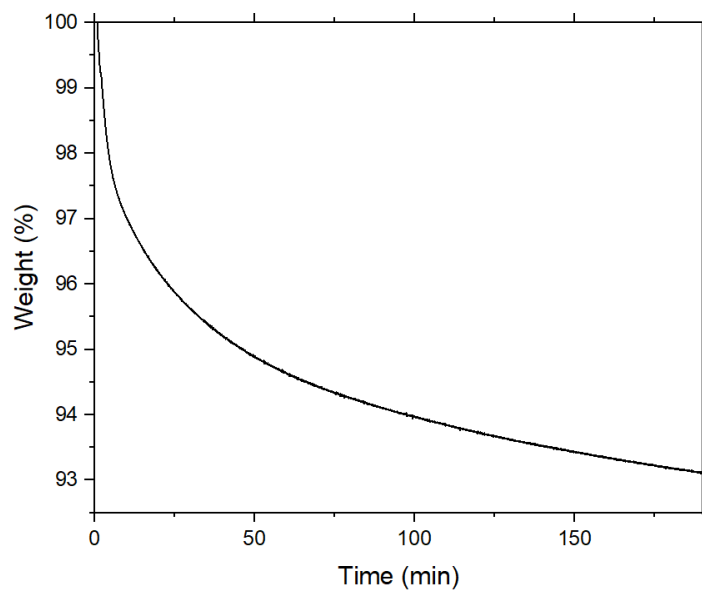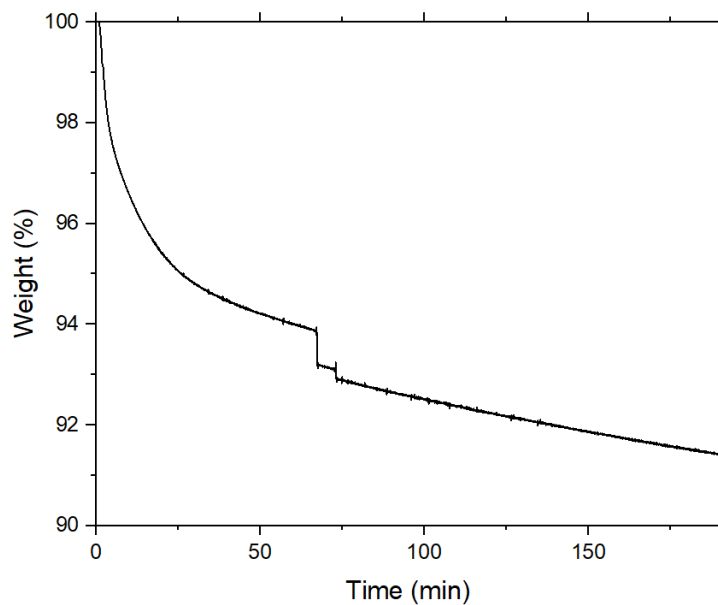

Figure A.10 (Isothermal TGA held at 425 °C)

Isothermal TGA of **P1** held at 425 °C for 3 hrs.
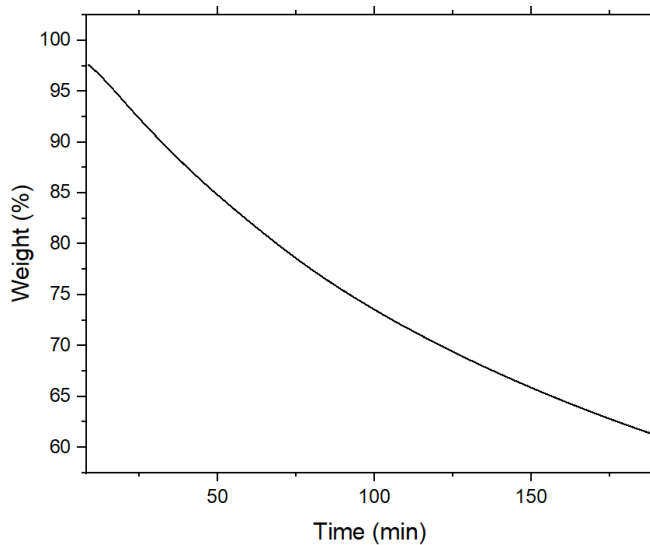
Figure A.11 (Isothermal TGA held at 450 °C)

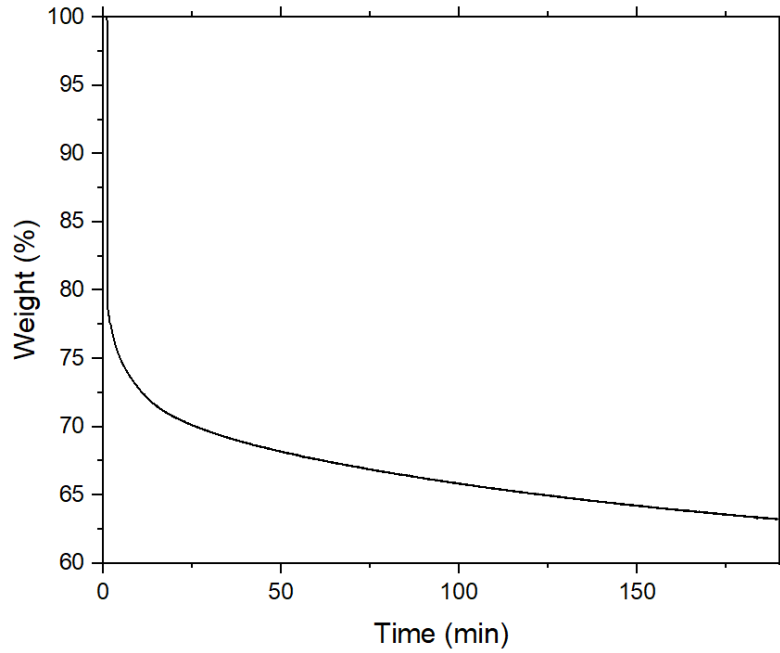Isothermal TGA of **P1** held at 450 °C for 3 hrs.

A.3.2   P2 PFCB-BP
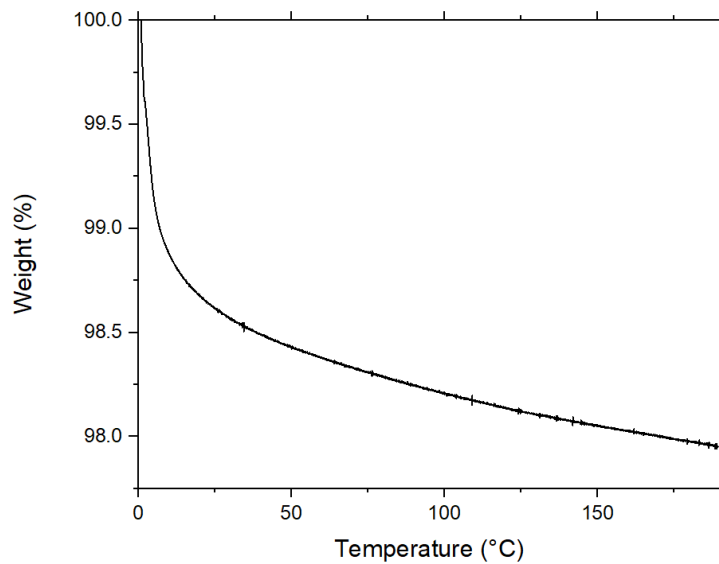
Figure A.12 (Isothermal TGA held at 360 °C)

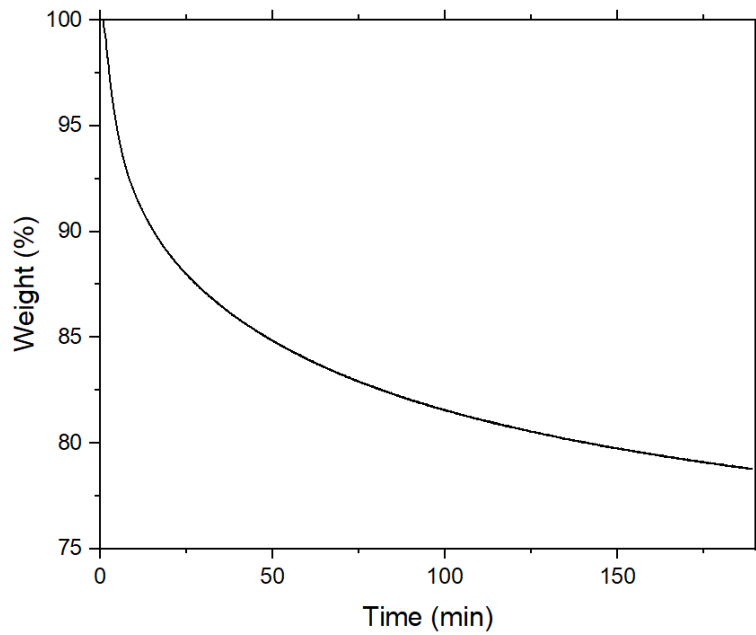Isothermal TGA of **P2** held at 360 °C for 3 hrs.
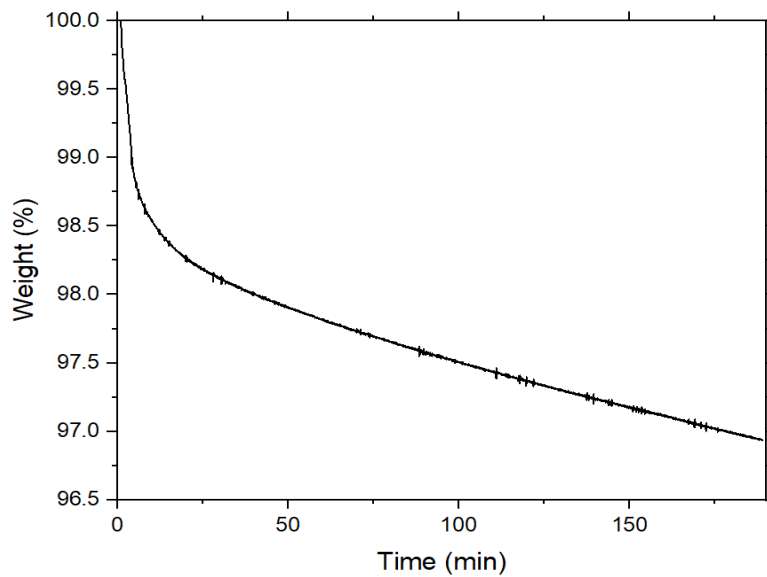
Figure A.13 (Isothermal TGA held at 380 °C)

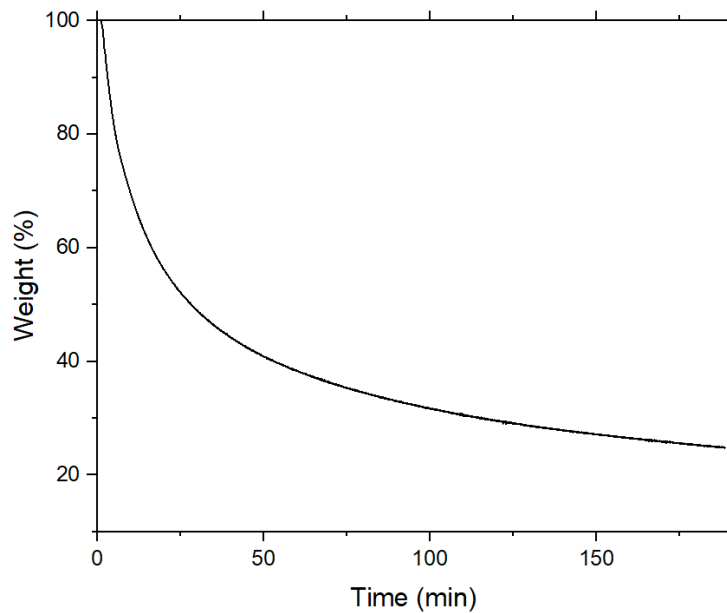Isothermal TGA of **P2** held at 380 °C for 3 hrs.
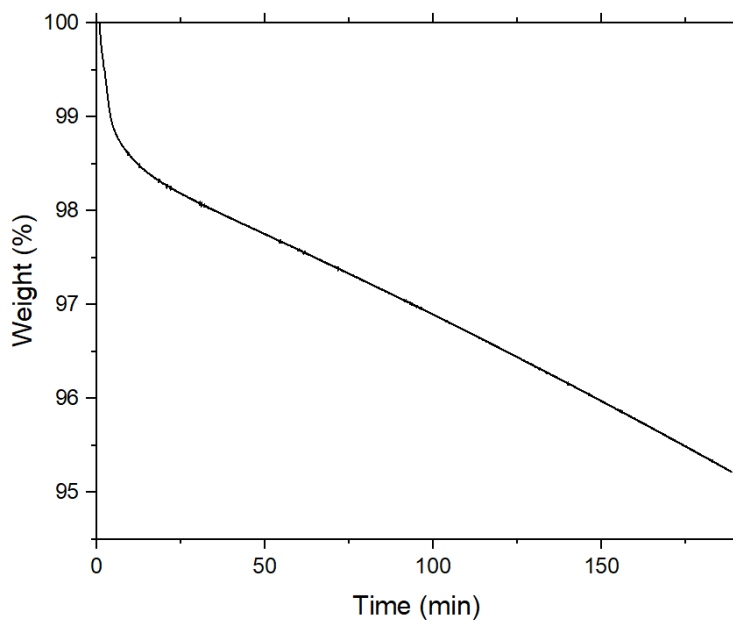
Figure A.14 (Isothermal TGA held at 400 °C)

Isothermal TGA of **P2** held at 400 °C for 3 hrs.
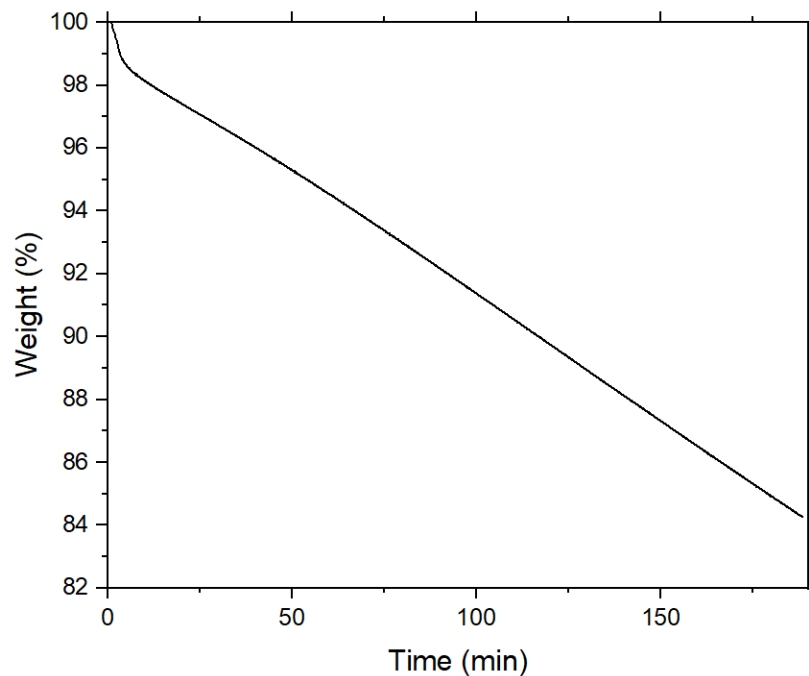
Figure A.15 (Isothermal TGA held at 420 °C)
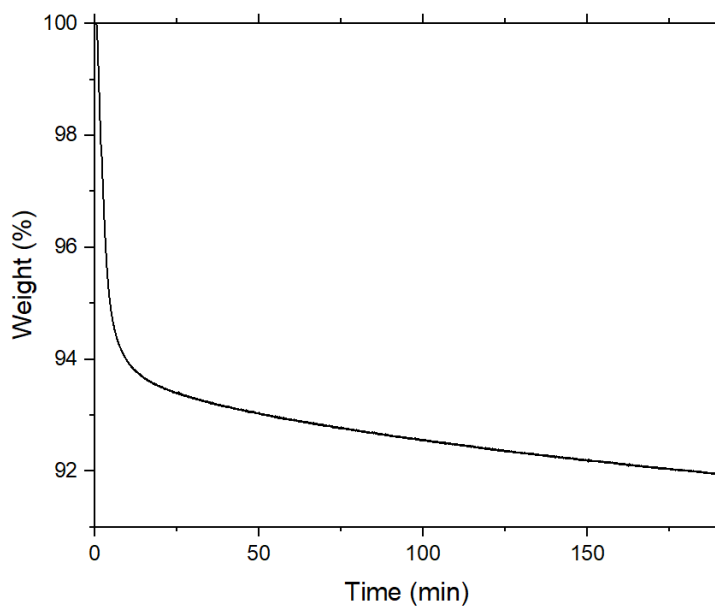
Isothermal TGA of **P2** held at 420 °C for 3 hrs.
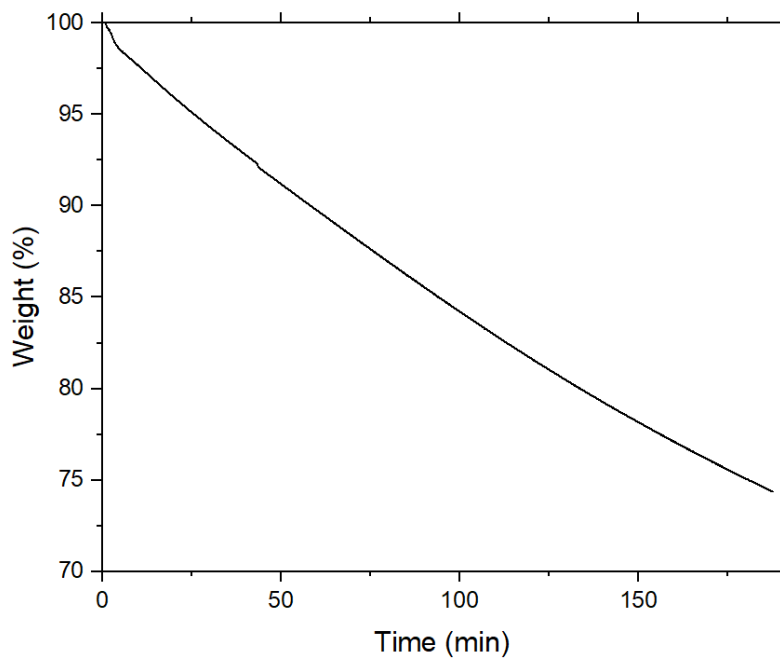
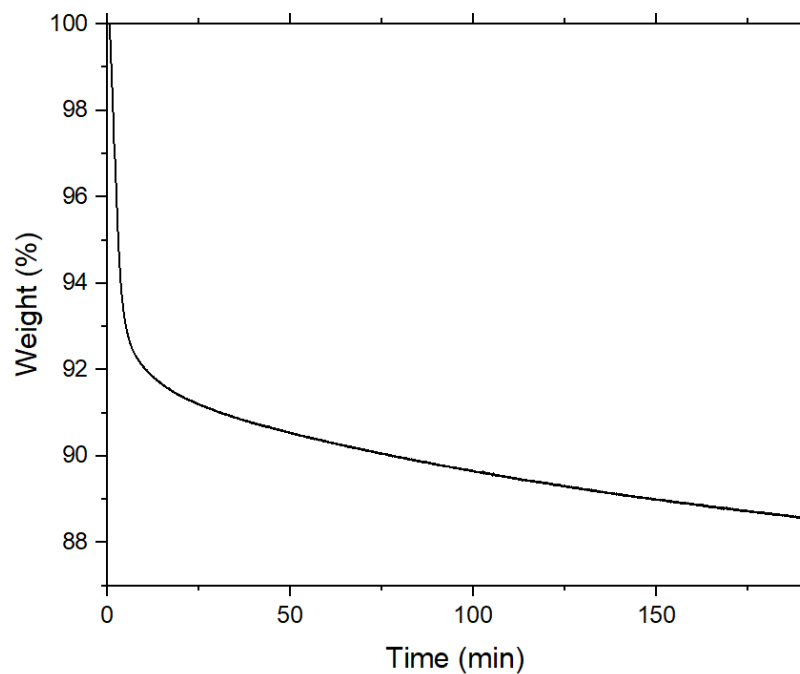

Figure A.16 (Isothermal TGA held at 440 °C)

Isothermal TGA of **P2** held at 440 °C for 3 hrs.
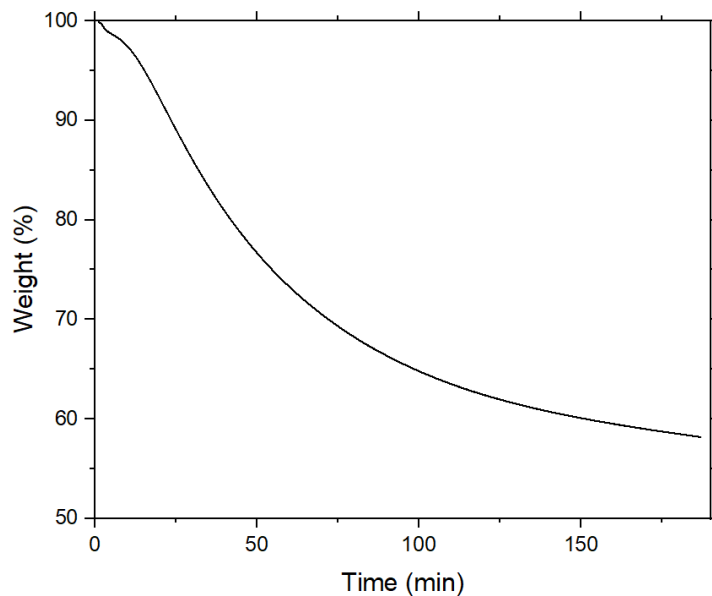
Figure A.17 (Isothermal TGA held at 460 °C)

Isothermal TGA of **P2** held at 460 °C for 3 hrs.

## A.3.3   P3 PFCA
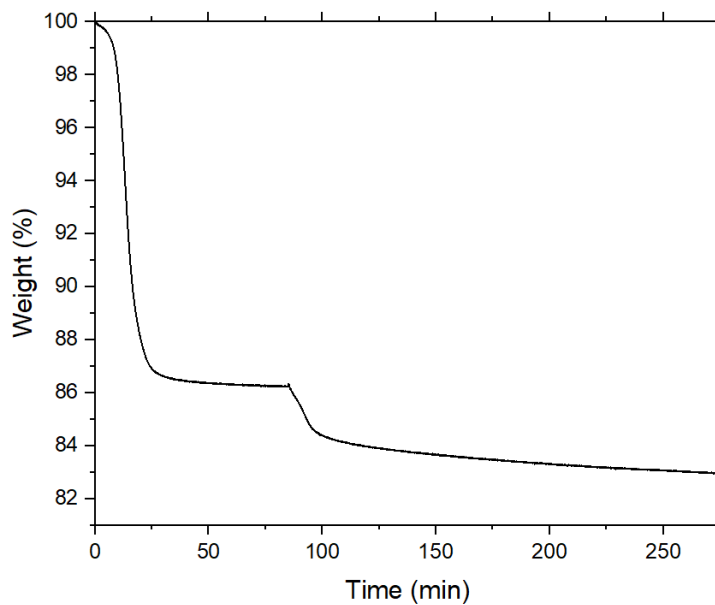
Figure A.18 (Isothermal TGA held at 370 °C)

Isothermal TGA of **P3** held at 250 °C for 1 hr. to fully polymerize then at 370 °C for 3 hrs.
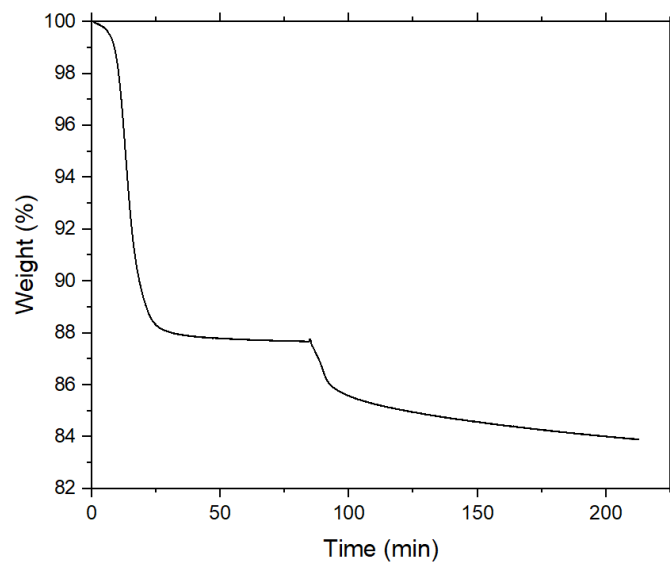
Figure A.19 (Isothermal TGA held at 390 °C)

Isothermal TGA of **P3** held at 250 °C for 1 hr. to fully polymerize then held at 390 °C for 3 hours.
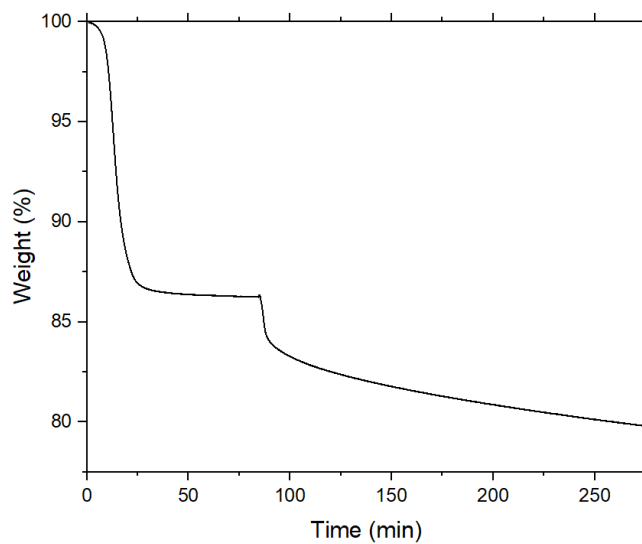
Figure A.20 (Isothermal TGA held at 410 °C)

Isothermal TGA of **P3** held at 250 °C for 1 hr. to fully polymerize then held at 410 °C for 3 hours.
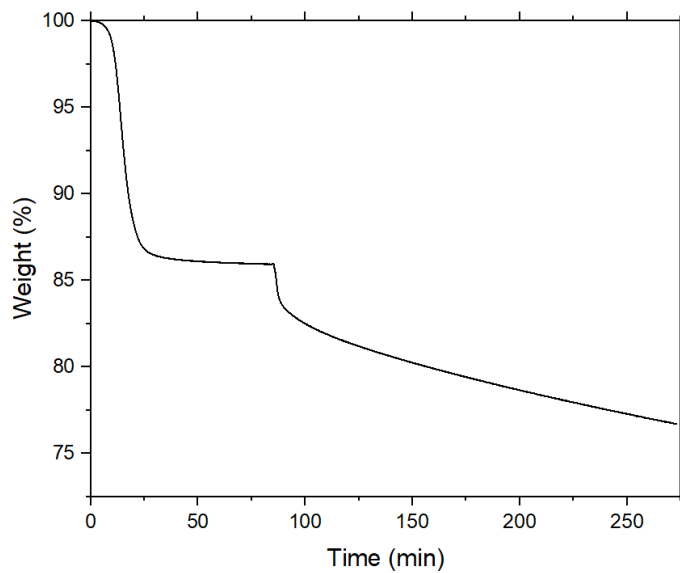
Figure A.21 (Isothermal TGA held at 430 °C)

Isothermal TGA of **P3** held at 250 °C for 1 hr. to fully polymerize then held at 430 °C for 3 hours.
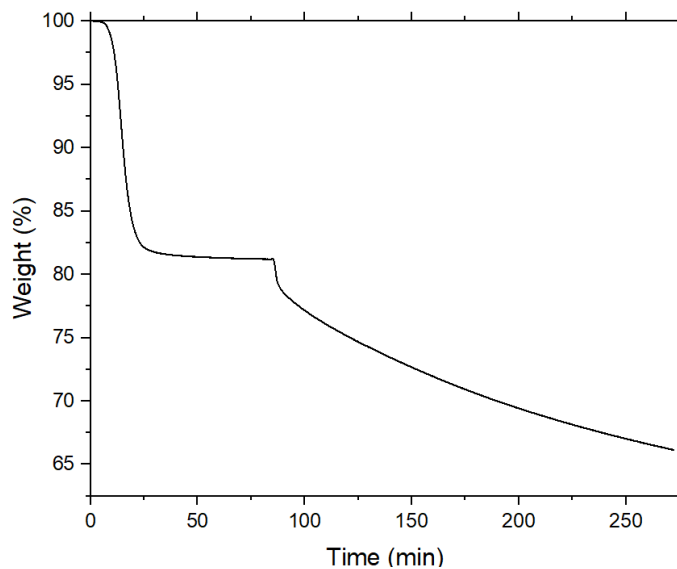
Figure A.22 (Isothermal TGA held at 450 °C)

Isothermal TGA of **P3** held at 250 °C for 1 hr. to fully polymerize then held at 450 °C for 3 hours.
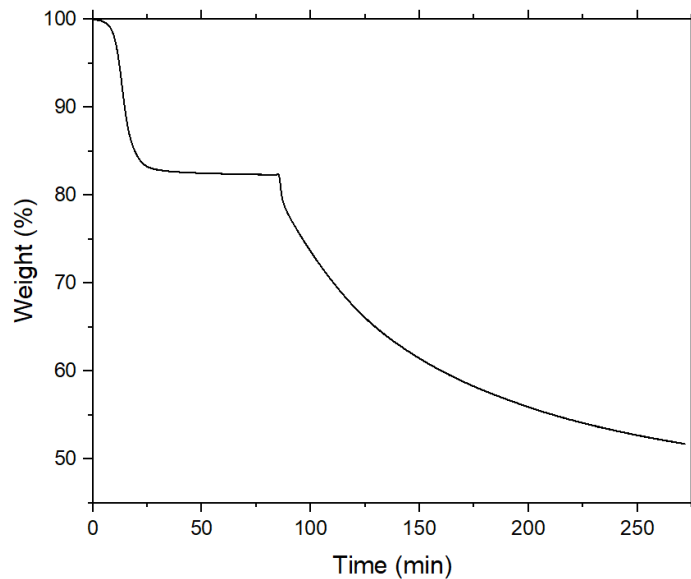
Figure A.23 (Isothermal TGA held at 470 °C)

Isothermal TGA of **P3** held at 250 °C for 1 hr. to fully polymerize then held at 470 °C for 3 hours.

A.3.4 P4 FAVE-Acenapthylenone

Figure A.24 (Isothermal TGA held at 300 °C)

Isothermal TGA of **P4** held at 300 °C for 3 hrs.

Figure A.25 (Isothermal TGA held at 320 °C)
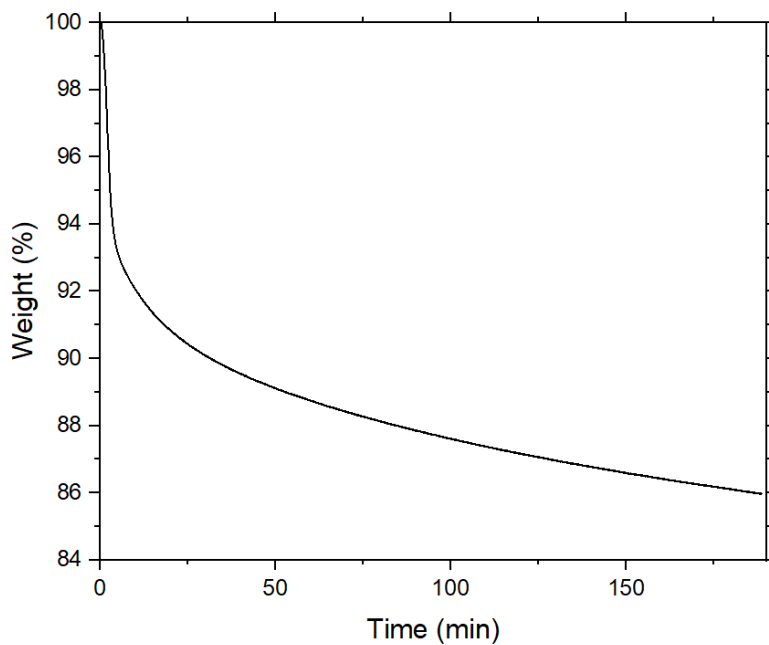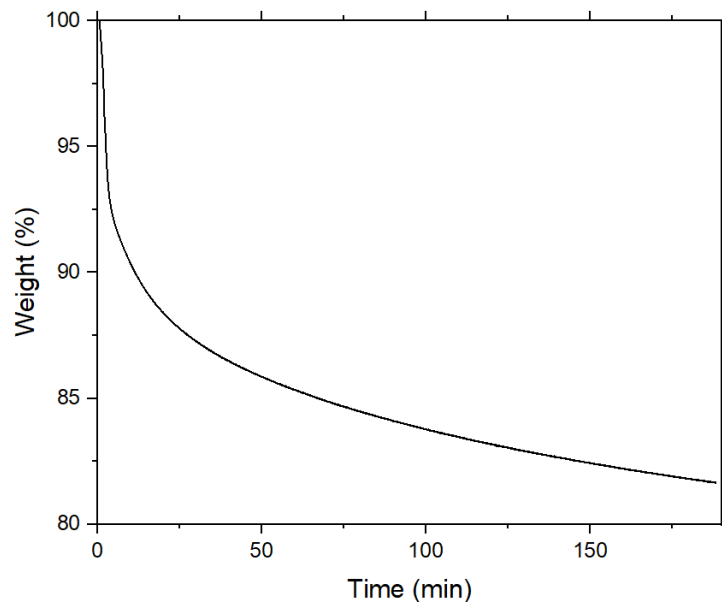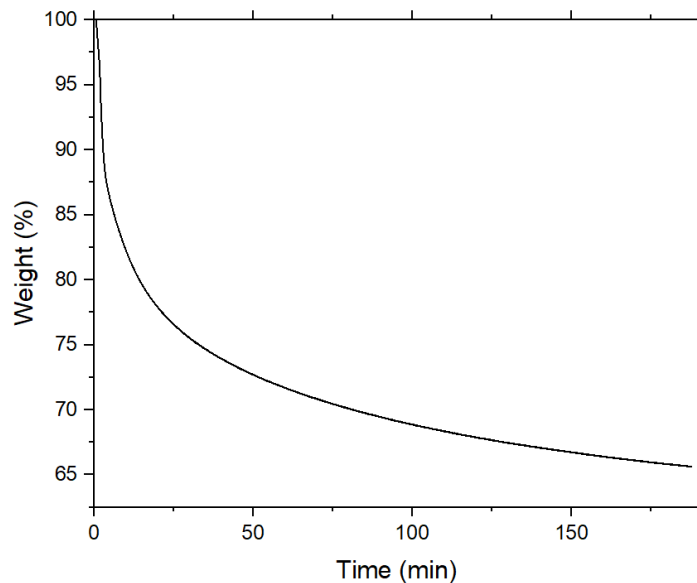
Isothermal TGA of **P4** held at 320 °C for 3 hrs.

Figure A.26 (Isothermal TGA held at 340 °C)

Isothermal TGA of **P4** held at 340 °C for 3 hrs.

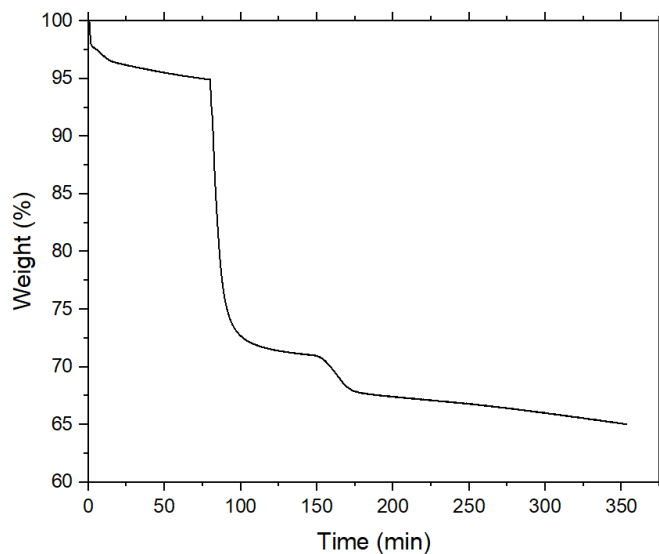Figure A.27 (Isothermal TGA held at 360 °C)

Isothermal TGA of **P4** held at 360 °C for 3 hrs.

Figure A.28 (isothermal TGA held at 380 °C)

Isothermal TGA of **P4** held at 380 °C for 3 hrs.

Figure A.29 (Isothermal TGA held at 400°C)

Isothermal TGA of **P4** held at 400 °C for 3 hrs.

A.3.5   P5 FAVE-Phenanthrenone

Figure A.30 (Isothermal TGA held at 340 °C)

Isothermal TGA of **P5** held at 340 °C for 3 hrs.

Figure A.31 (Isothermal TGA held at 360 °C)

Place Isothermal TGA of **P5** held at 360 °C for 3 hrs.
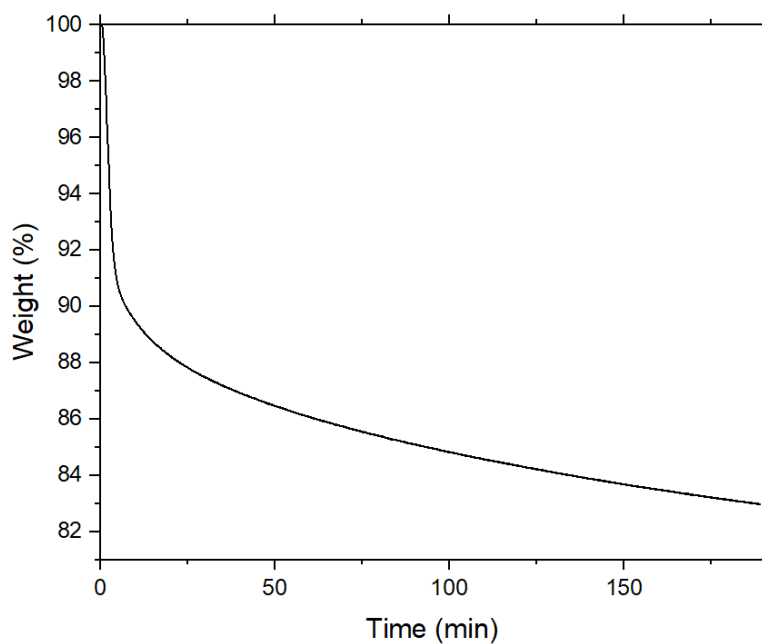
Figure A. 32 (Isothermal TGA held at 380 °C)

Isothermal TGA of **P5** held at 380 °C for 3 hrs.

Figure A.33 (Isothermal TGA held at 400 °C)

Isothermal TGA of **P5** held at 400 °C for 3 hrs.

Figure A. 34 (Isothermal TGA held at 420 °C)

Isothermal TGA of P5 held at 440 °C for 3 hrs.

Figure A.35 (Isothermal TGA held at 440 °C)

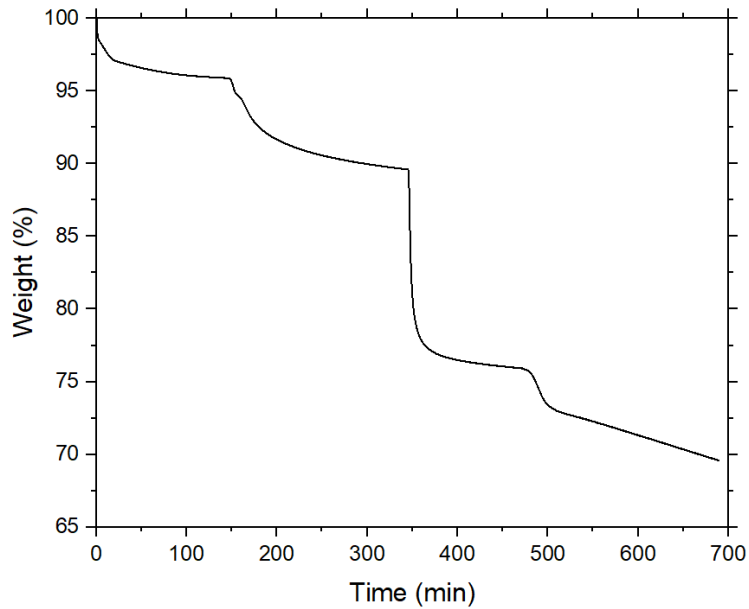Isothermal TGA of P5 held at 440 °C for 3 hrs.

A.3.6 P6 BODA-Ether

Figure A.36 (Isothermal TGA held at 400 °C and 1000 °C)

Isothermal TGA of P6 held at 250 °C for 1 hr. then held at 400 °C for 3 hrs. and 1000 °C for 3 hrs.
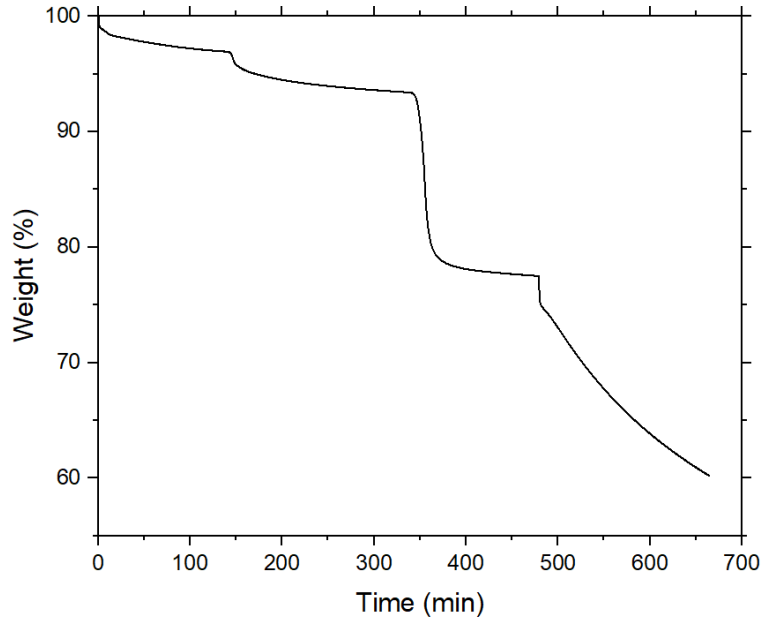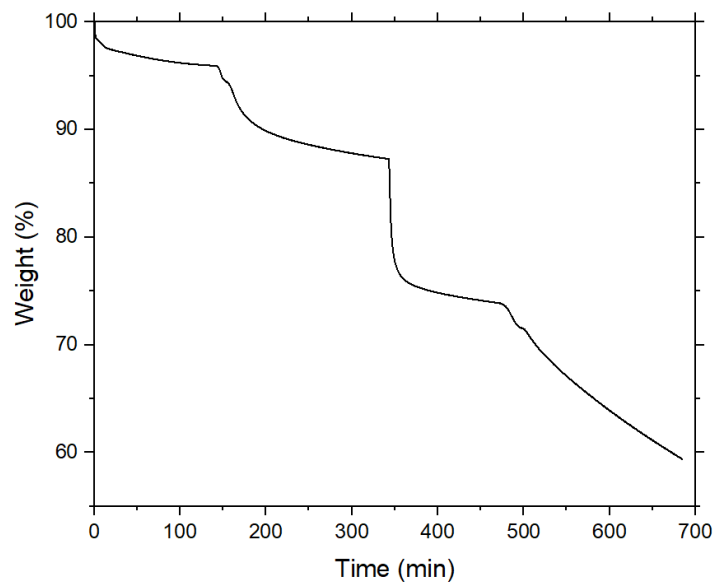
Figure A.37 (Isothermal TGA held at 420 °C and 980 °C)

Isothermal TGA of P6 held at 250 °C and 400 °C for 1 hr. each then held at 420 °C for 3 hrs. and 980 °C for 3 hrs.
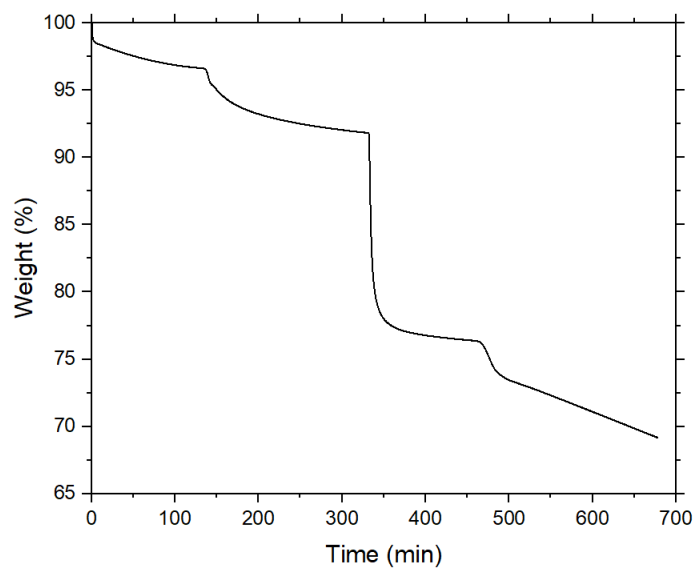

Figure A.38 (Isothermal TGA held at 440 °C and 960 °C)

Isothermal TGA of P6 held at 250 °C and 400 °C for 1 hr. each then held at 400 °C for 3 hrs. and 960 °C for 3 hrs.
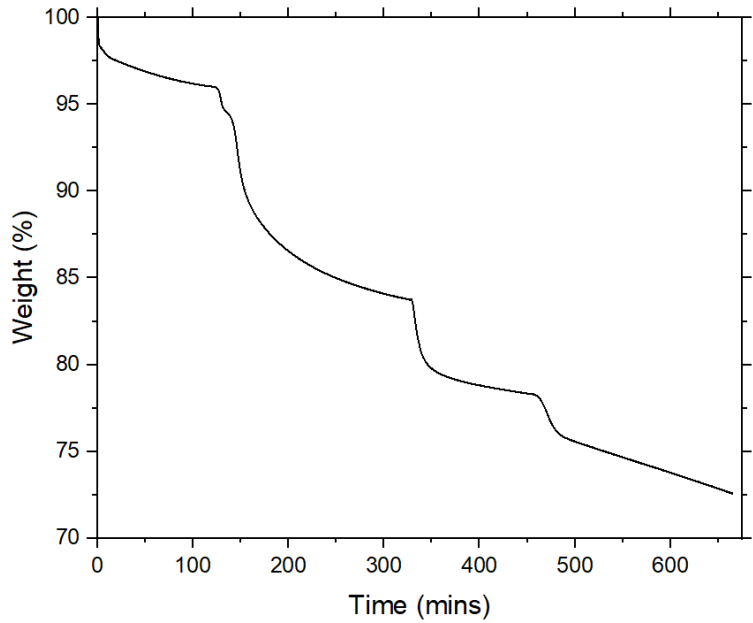
Figure A.39 (Isothermal TGA held at 460 °C and 940 °C)

Isothermal TGA of P6 held at 250 °C and 400 °C for 1 hr. each then held at 460 °C for 3 hrs. and 940 °C for 3 hrs.

Figure A.40 (Isothermal TGA held at 480 °C and 920 °C)

Isothermal TGA of P6 held at 250 °C and 400 °C for 1 hr. each then held at 480 °C for 3 hrs. and 920 °C for 3 hrs.

Figure A.41 (Isothermal TGA held at 500 °C and 900 °C)

Isothermal TGA of P6 held at 250 °C and 400 °C for 1 hr. each then held at 500 °C for 3 hrs. and 900 °C for 3 hrs.
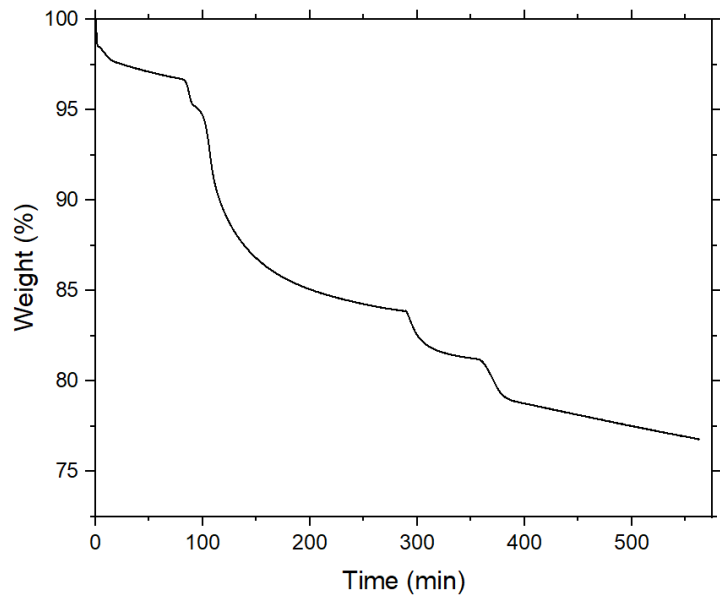

Figure A.42 (Isothermal TGA held at 520 °C and 880 °C)

Isothermal TGA of P6 held at 250 °C and 400 °C for 1 hr. each then held at 520 °C for 3 hrs and 880 °C for 3 hrs.
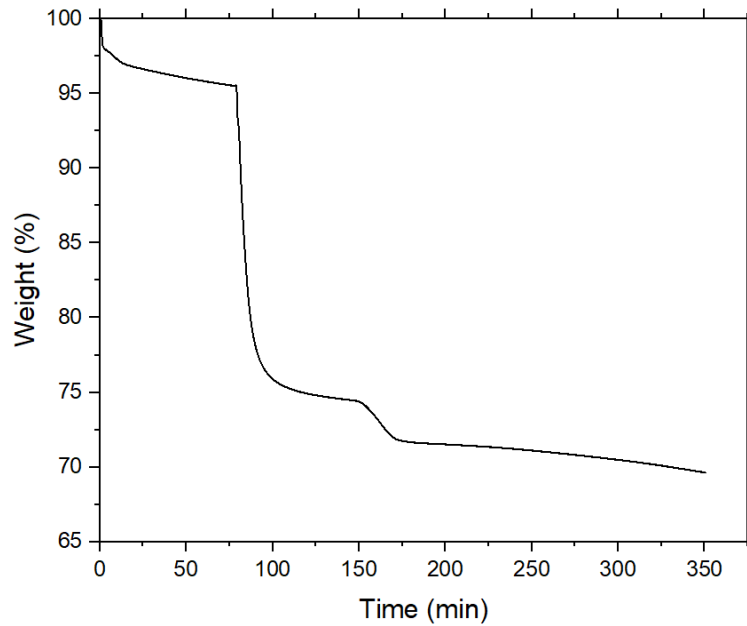
Figure A.43 (Isothermal TGA held at 860 °C)

Isothermal TGA of P6 held at 250 °C and 400 °C for 1 hr. each and then held at 860 °C for 3 hrs.
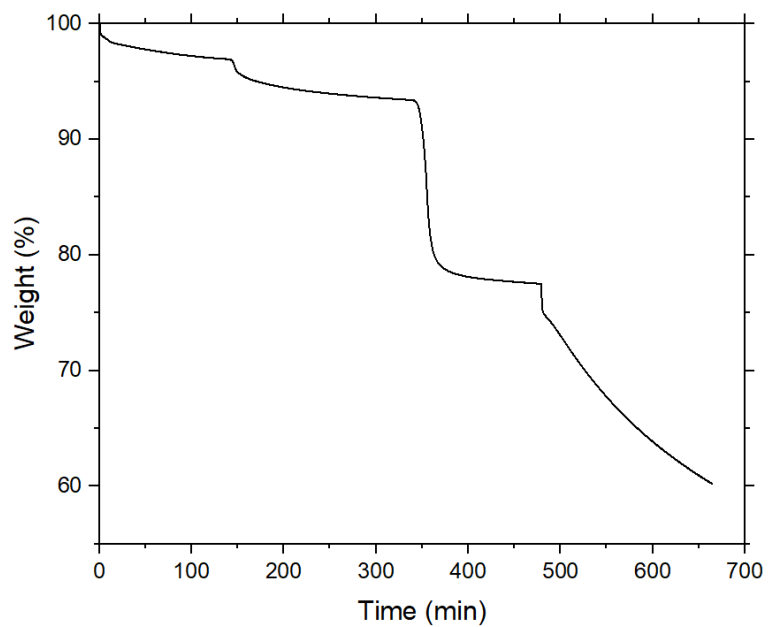

Figure A.44 (Isothermal TGA held at 840 °C)

Isothermal TGA of P6 held at 250 °C and 400 °C for 1 hr. each then held at 840 °C for 3 hrs.